**NASA Technical Paper 2850**

1989

# Partitioning Strategy for Efficient Nonlinear Finite Element Dynamic Analysis on Multiprocessor Computers

Ahmed K. Noor
and Jeanne M. Peters
*The George Washington University*
*Joint Institute for Advancement of Flight Sciences*
*Langley Research Center*
*Hampton, Virginia*



NASA
National Aeronautics
and Space Administration

**Scientific and Technical
Information Division**

The use of trademarks or names of manufacturers in this report is for accurate reporting and does not constitute an official endorsement, either expressed or implied, of such products or manufacturers by the National Aeronautics and Space Administration.

## Contents

## Symbols

| | |
|---|---|
| $E_L, E_T$ | elastic moduli of individual layers in direction of fibers and normal to it, respectively |
| $[F]$ | flexibility matrix (see eqs. (1)) |
| $[F_{11}], [F_{22}]$ | partitions of matrix $[F]$ |
| $[\bar{F}], [\tilde{F}]$ | components of matrix $[F]$ |
| $\{f_H\}, \{f_V\}$ | vectors (see eqs. (A7)) |
| $\{\bar{f}_H\}, \{\tilde{f}_H\}$ | components of vector $\{f_H\}$ |
| $\{\bar{f}_V\}, \{\tilde{f}_V\}$ | components of vector $\{f_V\}$ |
| $\{G(X)\}, \{N(H,X)\}$ | vectors of nonlinear terms (see eqs. (1) and (2)) |
| $G_{LT}, G_{TT}$ | shear moduli of individual layers in plane of fibers and normal to it, respectively |
| $\{G\}_1, \{G\}_2$ | partitions of vector $\{G\}$ |
| $\{H\}$ | vector of stress-resultant parameters |
| $\{H\}_1, \{H\}_2$ | partitions of vector $\{H\}$ |
| $h$ | total thickness of panel |
| $\overset{\star}{\mathrm{K}}$ | total kinetic energy of structure |
| $[K]$ | global structure matrix (see eqs. (4)) |
| $[K_V]$ | matrix defined in equations (A10) |
| $[K_{VV}], [K_{HV}], [K_{HH}]$ | matrices defined in equations (A12) to (A14) |
| $[\bar{K}], [\tilde{K}], [\bar{\bar{K}}], [\tilde{\bar{K}}], [\bar{\tilde{K}}], [\tilde{\tilde{K}}]$ | components of matrix $[K]$ (see eqs. (7) and (8)) |
| $[M]$ | consistent mass matrix (see eqs. (2)) |
| $[M_{11}], [M_{13}], [M_{22}], [M_{23}], [M_{33}]$ | partitions of matrix $[M]$ |
| $[\bar{M}], [\tilde{M}]$ | components of matrix $[M]$ |
| $m$ | number of time steps in multi-step one-derivative scheme (see eq. (A1)) |
| m | integer which depends on number of symmetry operations used |
| $\{N\}_1, \{N\}_2, \{N\}_3$ | partitions of vector $\{N\}$ |
| $\{P\}$ | vector of external forces |
| $p_o$ | intensity of normal loading |
| $\{Q\}$ | right-hand side vector (see eqs. (4)) |
| $\{Q_V\}$ | vector defined in equation (A11) |
| $\{Q\}_1, \{Q\}_2, \{Q\}_3$ | partitions of vector $\{Q\}$ |
| $\{\bar{Q}\}, \{\tilde{Q}\}, \{\bar{\bar{Q}}\}, \{\tilde{\bar{Q}}\}, \{\bar{\tilde{Q}}\}, \{\tilde{\tilde{Q}}\}$ | components of vector $\{Q\}$ (see eqs. (7) and (8)) |
| $\{\bar{\bar{R}}\}, \{\tilde{\bar{R}}\}, \{\bar{\tilde{R}}\}, \{\tilde{\tilde{R}}\}$ | symmetric/antisymmetric components of residual vectors used in PCG technique |
| R | radius of curvature of cylindrical panel |
| $[S]$ | strain-displacement matrix (see eqs. (2)) |
| $S_T$ | total speedup obtained by using proposed strategy |
| $[S_{11}], [S_{13}], [S_{22}], [S_{23}]$ | partitions of matrix $[S]$ |

| | |
|---|---|
| $[\bar{S}], [\tilde{S}]$ | components of matrix $[S]$ |
| $[T_H], [T_V], [T_X]$ | transformation matrices (see eqs. (B15) to (B19)) |
| $[\bar{T}_H], [\tilde{T}_H], [\bar{T}_X], [\tilde{T}_X], [\bar{T}_Q], [\tilde{T}_Q]$ | matrices defined in equations (B11) to (B14) |
| $[\bar{T}_V], [\tilde{T}_V]$ | transformation matrices (see eqs. (6)) |
| $t$ | time |
| $U^c$ | total complementary strain energy of structure |
| $u_1, u_2, w$ | displacement components of middle surface of shell in coordinate directions |
| $\{V\}$ | vector of nodal velocities |
| $\{V\}_1, \{V\}_2, \{V\}_3$ | partitions of vector $\{V\}$ |
| $\{X\}$ | vector of nodal displacements |
| $\{X\}_1, \{X\}_2, \{X\}_3$ | partitions of vector $\{X\}$ |
| $x_1, x_2, x_3$ | orthogonal coordinate system |
| $\{\bar{\bar{Y}}\}, \{\tilde{\bar{Y}}\}, \{\bar{\tilde{Y}}\}, \{\tilde{\tilde{Y}}\}$ | symmetric/antisymmetric components of residual vectors used in PCG technique |
| $\{\bar{\bar{Z}}\}, \{\tilde{\bar{Z}}\}, \{\bar{\tilde{Z}}\}, \{\tilde{\tilde{Z}}\}$ | symmetric/antisymmetric components of conjugate search direction vectors |
| $\alpha_i, \beta_i$ | coefficients in multistep operators (see table AI) |
| $\bar{\alpha}_j$ | step length for $j$th correction vector of PCG technique |
| $\bar{\beta}_{j+1}$ | orthogonalization coefficient used in $j$th iteration of PCG technique |
| $[\Gamma_s], [\Gamma_a]$ | transformation matrices |
| $\Delta t$ | time step used in temporal integration scheme |
| $\varepsilon$ | prescribed tolerance in PCG technique |
| $\lambda_0, \lambda_1, \lambda$ | tracing parameters identifying correction terms to symmetric response vectors |
| $\upsilon_{LT}$ | major Poisson's ratio of individual layers of panel |
| $\phi_1, \phi_2$ | rotation components of middle surface of panel |
| $\{\psi\}$ | vector of stress parameters and nodal velocities |
| $\{\bar{\bar{\psi}}\}, \{\tilde{\bar{\psi}}\}, \{\bar{\tilde{\psi}}\}, \{\tilde{\tilde{\psi}}\}$ | symmetric/antisymmetric components of vector $\{\psi\}$ |
| $\Omega, \hat{\Omega}$ | original and effective element domains (see fig. 1) |

Subscripts:

| | |
|---|---|
| $a$ | antisymmetric component |
| $i$ | time |
| $j$ | PCG iteration cycle |
| max | maximum value |
| $p, q$ | range from 1 to total number of nodal velocities in model |
| p | ranges from 1 to total number of stress-resultant parameters in model |

| | |
|---|---|
| $s$ | symmetric component |
| Superscripts: | |
| $(r)$ | Newton-Raphson iteration cycle |
| $T$ | transposition |
| Abbreviations: | |
| CP | central processor |
| CPU | central processing unit |
| ECL | emitter coupled logic |
| MFLOPS | millions of floating point operations per second |
| PCG | preconditioned conjugate gradient |

A dot over a symbol indicates a derivative with respect to time; a bar ($\bar{}$) over a vector refers to symmetric components; a tilde ($\tilde{}$) over a vector refers to antisymmetric components.

## Abstract

A computational procedure is presented for the nonlinear dynamic analysis of unsymmetric structures on vector multiprocessor systems. The procedure is based on a novel hierarchical partitioning strategy in which the response of the unsymmetric structure at any time instant is approximated by a linear combination of symmetric and antisymmetric response vectors, each obtained by using only a fraction of the degrees of freedom of the original finite element model. The three key elements of the procedure which result in a high degree of concurrency throughout the solution process are (1) mixed (or primitive variable) formulation with independent shape functions for the different fields, (2) operator splitting or restructuring of the discrete equations at each time step to delineate the symmetric and antisymmetric vectors constituting the response, and (3) two-level iterative process for generating the response of the structure. An assessment is made of the effectiveness of the procedure on the CRAY X-MP/4 computers.

## 1. Introduction

Dynamic response calculations for future aerospace systems are expected to require processing rates far in excess of the upper limit of computers built around a single processing unit. This is because of the complexity of these systems and the high degree of sophistication of the computational models required for simulating their response (see, for example, ref. 1). The introduction of novel forms of machine architecture has brightened the prospects for meeting future large-scale computational needs. Most of the new machines achieve high performance through vectorization and/or parallelism. These include top-of-the-range supercomputers such as CRAY X-MP, CRAY 2, and ETA-10, as well as computers based on readily available and inexpensive basic units such as the hypercubes and the Connection Machine. The characteristics of several new machines are summarized in references 2 to 5.

Much work has been devoted to the development of vector and parallel numerical algorithms for performing matrix operations, solution of algebraic equations, and extraction of eigenvalues. (See, for example, refs. 6 to 10.) Also, a number of special strategies have been proposed for increasing the degree of parallelism and/or vectorization in finite element computations. These strategies include domain decomposition (or substructuring), operator splitting, and element-by-element techniques. They are related to the "divide and conquer" paradigm based on breaking a large (complex) problem into a number of smaller (simpler) subproblems which may be solved independently on distinct processors. The degree of independence of the subproblems is a measure of the effectiveness of the algorithm since it determines the amount and frequency of communication and synchronization.

Substructuring techniques when combined with operator splitting and iterative procedures result in computational strategies which are well-suited for parallel vectorization. (See refs. 11 and 12.) However, for the strategy to be effective the following two conditions must be satisfied:

1. The partitioning of a discretized structure into substructures must achieve well-balanced workload distribution among the different processors.

2. The iterative process used to account for the coupling between the different substructures must be rapidly converging. This, in turn, requires the substructures not to be strongly coupled.

The two conditions are difficult to satisfy, and to date, despite a number of attempts to develop partitioning strategies (see, for example, refs. 13 and 14), no general strategy exists which satisfies the aforementioned two conditions. The present study focuses on this problem. Specifically, the objective of this paper is to present an effective hierarchical partitioning strategy for use in large-scale nonlinear finite element dynamic analysis on multiprocessor computers. To sharpen the focus of the study, multiprocessor computers with a small number of powerful processors such as the CRAY X-MP/4 are considered.

The authors had useful discussions with Huey Carden of NASA Langley Research Center, Ahmed Sameh of the University of Illinois at Urbana-Champaign, and Chris Hsiung of CRAY Research, Inc., Chippewa Falls, Wisconsin. Also, Phuong H. Vu and Richard Steimann of CRAY Research, Inc., Mendota Heights, Minnesota, helped in the computer
implementation.

## 2. Mathematical Formulation

The analytical formulation is based on a moderate-rotation geometrically nonlinear theory of the structure. (See ref. 15.) All the dissipative forces are neglected. A mixed formulation is used in which the fundamental unknowns consist of the internal forces (or stress resultants), the generalized displacements, and the velocity components of the structure. A total Lagrangian description of the deformation of the structure is used, in which the configurations of the structure at different times are referred to the initial coordinate system of the undeformed structure.

The spatial discretization is performed by dividing the structure into finite elements. The degree of

the polynomial shape functions used for approximating the generalized displacements and velocity components differs from the degree of the polynomials used in approximating the stress resultants. Moreover, continuity of stress resultants is not imposed at interelement boundaries. The semidiscrete system of equations governing the dynamic response of the structure consists of the following three sets of relations:

*Constitutive relations:*

$$[F]\{H\} = [S]\{X\} + \{G(X)\} \tag{1}$$

*Equations of motion:*

$$[M]\{\dot{V}\} = \{P\} - [S]^T\{H\} - \{N(H,X)\} \tag{2}$$

*Relations between velocity and displacement components:*

$$\{\dot{X}\} = \{V\} \tag{3}$$

where $\{X\}$ and $\{V\}$ are the vectors of unknown nodal displacements and velocities, respectively; $\{H\}$ is the vector of stress-resultant parameters; $[F]$ is a block diagonal matrix of element flexibilities (with each diagonal block associated with the flexibility matrix of a single element); $[S]$ is the linear strain-displacement matrix; $\{P\}$ is the vector of external forces; $[M]$ is a banded matrix of the consistent mass coefficients; $\{G(X)\}$ and $\{N(H,X)\}$ are the vectors of nonlinear terms; superscript $T$ denotes transposition; and a dot over the symbol indicates a derivative with respect to time. In the moderate-rotation theory used herein, the vector $\{G(X)\}$ is quadratic in $\{X\}$; and the vector $\{N(H,X)\}$ is bilinear in $\{H\}$ and $\{X\}$.

The temporal integration is performed by using an implicit, multistep, one-derivative scheme. The resulting nonlinear simultaneous algebraic equations at each time step are solved by using a Newton-Raphson iterative technique. The iterative process is represented by the following equations for the stress parameters and velocity components of the $r$th iteration cycle (see appendix A):

$$[K]_i^{(r)}\{\Delta\psi\}_i^{(r)} = \{Q\}_i^{(r)} \tag{4}$$

$$\{\psi\}_i^{(r+1)} = \{\psi\}_i^{(r)} + \{\Delta\psi\}_i^{(r)} \tag{5}$$

where $[K]_i^{(r)}$ is a global structure matrix which includes the flexibility $[F]$, linear strain displacement $[S]$, mass $[M]$, and nonlinear contributions $\{G(X)\}$ and $\{N(H,X)\}$ from different elements (see appendix A); $\{Q\}_i^{(r)}$ is the global right-hand side vector; and $\{\psi\}_i^{(r+1)} = \left\{\begin{matrix}H\\V\end{matrix}\right\}_i^{(r+1)}$ are the stress parameters and velocity components at the end of the $r$th iteration cycle at time $i$. The procedure for evaluating the corresponding nodal displacements, $\{X\}_i^{(r+1)}$, is outlined in appendix A.

## 3. Basic Idea and Key Elements of the Proposed Procedure

The proposed procedure is based on approximating the response of the unsymmetric structure, at any time instant, by a linear combination of symmetric and antisymmetric response vectors (or modes). Each of these modes is generated with the use of a reduced-size model of the original structure. The size of the reduced model depends on the number of symmetry operations used.

The model-size reduction process is depicted in figures 1 and 2. It can be thought of as a hierarchical partitioning strategy, in which the original structure is replaced by an equivalent symmetrized structure, having the same symmetric/antisymmetric components of the response.

The top left sketch in figure 1 shows the original unsymmetric finite element model. The response vector $\{V\}$ is decomposed into symmetric and antisymmetric vectors $\{V\}_s$ and $\{V\}_a$ with respect to line ab. (See fig. 2.) Each pair of complementary elements (with respect to ab) is replaced by a single effective element in the symmetrized structure. Since each of the symmetric and antisymmetric components of the response vector is generated by using only one half the symmetrized structure, the decomposition process amounts to partitioning the original structure into two substructures.

The process is repeated to effect further reduction in the size of the substructures by decomposing each of the vectors $\{\bar{V}\}_s$ and $\{\tilde{V}\}_a$ into symmetric/antisymmetric subvectors with respect to line cd in figure 1. Each of the resulting four vectors $\{\bar{\bar{V}}\}$, $\{\tilde{\bar{V}}\}$, $\{\bar{\tilde{V}}\}$, and $\{\tilde{\tilde{V}}\}$ can be generated by using only one quadrant of the symmetrized structure (shown in the bottom right sketch of fig. 1). Henceforth, a bar ($^-$) and a tilde ($^\sim$) over a vector refer to the symmetric and antisymmetric components of the vector, respectively.

If the fundamental unknowns are selected to be the symmetric/antisymmetric components of the response vector, the governing equations in these unknowns can be obtained by using simple matrix transformations on pairs of complementary elements (see appendix B). For symmetric structures, the governing equations in the symmetric/antisymmetric components of the response vector are uncoupled.

On the other hand, for unsymmetric structures, the equations are coupled. In the proposed procedure, the uncoupled equations are used as a preconditioner, and the coupling is accounted for by using an iterative process.

The three key elements of the proposed procedure are (1) mixed (primitive variable) formulation with independent shape functions for the stress resultants, generalized displacements, and velocity components, and with the stress resultants allowed to be discontinuous at interelement boundaries; (2) operator splitting or restructuring of the discrete equations of the structure to delineate the contributions to the symmetric and antisymmetric vectors constituting the response; and (3) two-level iterative process (with nested iteration loops) to generate the symmetric and antisymmetric components of the response vectors at each time step. The top- and bottom-level iterations (outer and inner iteration loops) are performed by using Newton-Raphson and preconditioned conjugate gradient (PCG) techniques, respectively.

## 4. Computational Procedure

A flowchart of the computational procedure is given in table I. The application of the proposed procedure to structural dynamics problems can be conveniently divided into two phases, each of which is well-suited for parallel processing:

1. *Preprocessing phase* in which the finite element model of the entire structure is used. The major steps in this phase are hierarchical partitioning of the response vectors, introducing the various transformation matrices (see appendix B and ref. 16), application of operator splitting, and generation of the various arrays for the reduced-size model through successive use of pairs of complementary elements from the model. (See fig. 1.) The number of degrees of freedom in the reduced-size model is approximately 1/m that of the original finite element model, where m is an integer which depends on the number of symmetry operations used. For the sake of load balancing, it is desirable to select the symmetries such that m equals the number of processors (i.e., 4 for the CRAY X-MP/4).

2. *Solution phase* is which only the reduced-size model is used in generating the transient response of the structure. The fundamental unknowns in this phase are the velocity components, stress resultants, and generalized displacements of one of the substructures.

A two-level iterative process (with two nested iteration loops) is used to generate the symmetric/antisymmetric components of the response vectors at each time step. The top-level iteration (outer iteration loop) is the Newton-Raphson iteration, and the bottom-level iteration (inner iteration loop) is the PCG iteration. The details of the PCG iterations are given in appendix C.

The following comments regarding the procedure seem to be in order:

1. The decomposition of the response vectors into symmetric and antisymmetric components can be performed by means of matrix transformations. For example, the symmetric and antisymmetric components of the velocity vector can be expressed as follows (see fig. 2):

$$\left.\begin{array}{ll} \{V\}_s = [\bar{T}_V]_1\{V\} & \{V\}_a = [\tilde{T}_V]_1\{V\} \\ \{V\}_{s,s} = [\bar{T}_V]_2\{\bar{V}\}_s & \{V\}_{s,a} = [\tilde{T}_V]_2\{\bar{V}\}_s \\ \{V\}_{a,s} = [\bar{T}_V]_2\{\tilde{V}\}_a & \{V\}_{a,a} = [\tilde{T}_V]_2\{\tilde{V}\}_a \end{array}\right\} \quad (6)$$

The symmetry transformations and the explicit form of the transformation matrices $[\bar{T}_V]$ and $[\tilde{T}_V]$ are given in appendix B.

2. The aforementioned transformations are used in conjunction with the operator splitting technique to delineate the different symmetric and antisymmetric components of the response. For the case of one symmetric operation (m = 2), equations (4) can be cast as

$$\left[[\bar{K}] + \lambda_0[\tilde{K}]\right]\{\Delta\psi\} = \{\bar{Q}\} + \lambda_0\{\tilde{Q}\} \quad (7)$$

where the subscript $i$ and the superscript $(r)$ are dropped for convenience. Similarly, for the case of two symmetry operations (m = 4), equations (4) can be cast as

$$\left[[\bar{\bar{K}}] + \lambda_1[\tilde{\bar{K}}] + \lambda_0\left([\bar{\tilde{K}}] + \lambda_1[\tilde{\tilde{K}}]\right)\right]\{\Delta\psi\}$$

$$= \{\bar{\bar{Q}}\} + \lambda_1\{\tilde{\bar{Q}}\} + \lambda_0\left(\{\bar{\tilde{Q}}\} + \lambda_1\{\tilde{\tilde{Q}}\}\right) \quad (8)$$

Tracing parameters $\lambda_0$ and $\lambda_1$ are introduced in equations (7) and (8) to identify the correction terms to the symmetric response vectors. The case $\lambda_0 = 0$ in equations (7) corresponds to a symmetric response with respect to ab (see fig. 1), and the case $\lambda_0 = \lambda_1 = 0$ in equations (8) corresponds to a symmetric response with respect to both cb and cd. For $\lambda_0 = \lambda_1 = 1$, equations (7) and (8) are equivalent to equations (4). Therefore, $\lambda_0$ and $\lambda_1$ are tracing parameters which identify all the coupling terms to the symmetric/antisymmetric components of the response vectors. The explicit forms of the arrays $[\bar{K}], [\tilde{K}], \{\bar{Q}\}$, and $\{\tilde{Q}\}$ in equations (7) are given in

appendix B (eqs. (B22) to (B25)). The vector $\{\Delta\psi\}$ refers to the increments of the symmetric and the antisymmetric components of the response vector. As shown in appendix B, the equations associated with each of the symmetric and antisymmetric components of the response vector are the same, except for the terms associated with the unknowns at the interfaces. Therefore, only one set of these equations needs to be considered. The sizes of the arrays in equations (7) are approximately 1/2 in the original equations (eqs. (4)). Similarly, the sizes of the arrays in equations (8) are approximately 1/4 the size of the corresponding ones in equations (4).

3. Equations (8) (or (7)) are solved by using the preconditioned conjugate gradient (PCG) technique. The matrix $[\bar{\bar{K}}]$ (or $[\bar{K}]$) is selected as the preconditioning matrix. For the case m = 4, the preconditioning matrix needs to be decomposed four times corresponding to the four different combinations of symmetry and antisymmetry conditions along cb and cd (see fig. 1). The four decompositions are done concurrently on different processors (whenever possible).

4. The preconditioned residuals in the PCG technique have regular, predetermined patterns of symmetry and antisymmetry with respect to cb and cd. These patterns are exploited in the solution process, in reducing the amount of computations, as well as in balancing the computational load between processors.

For the case m = 2, the procedure for generating the matrices $[\bar{K}], [\tilde{K}], \{\bar{Q}\}$, and $\{\tilde{Q}\}$ is outlined in appendix B and reference 16. The matrices for the case m =4 are obtained by repeating the same process as that used for m = 2.

## 5. Implementation on CRAY X-MP Computers

The proposed computational procedure based on hierarchical partitioning has been implemented on the CRAY X-MP/4 computer system at Cray Research, Inc., Mendota Heights, Minnesota. The major characteristics of the computer system are summarized in appendix D. The program was coded in FORTRAN using Cray FORTRAN (CFT) compiler directives for vectorization.

To improve the performance an attempt was made to maximize the use of the chaining facility of the CRAY computer (overlapping vector multiply, add, and memory access) whenever possible (steps 5, 6, 7, 8, and 11 of table I). This was accomplished by calling the SCILIB routines for performing the following six matrix/vector operations:

$$\begin{aligned}
&\text{SMXPY}: && \{Y\} + [M]\{X\} \\
&\text{SXMPY}: && \{Y\} + [M]^T\{X\} \\
&\text{MXV}: && [M]\{X\} \\
&\text{MXVA}: && [M]^T\{X\} \\
&\text{MXM}: && [M][A] \\
&\text{MXMA}: && [M]^T[A]
\end{aligned}$$

where $[M], [A]$ are matrices; $\{X\}, \{Y\}$ are vectors; and superscript $T$ denotes transposition.

The decomposition and back substitution in steps 10 and 11 (table I) were performed by using optimized versions of the LINPACK routines SPBFA and SPBSL which make extensive use of the chaining facility of the CRAY computer and have their innermost loops coded in assembly language. (See refs. 17 and 18.)

Multiprocessing was achieved by using the microtasking facility of the CRAY X-MP computer. This was accomplished by placing special directives in the code, then passing the code through a utility preprocessor called PREMULT to interpret these directives, and inserting the appropriate microtasking code. The output from PREMULT is then passed through the CFT compiler. The microtasking directives select the maximum number of CPU's to be used, identify the routines and DO loops to be microtasked, and identify the synchronization points in the code. The details of these directives are given in references 19, 20, and 21. In the proposed procedure, microtasking was used in steps 2, 5, 6, 7, 8, 10, and 11 of table I. Synchronization was used in steps 11 and 12. To increase the speedup gain from multiprocessing, microtasking was done on the outerloops of each of the aforementioned steps in table I, and therefore, the full arrays (elemental and structure arrays) were processed by each CPU, rather than dividing each of these arrays between the different CPU's.

## 6. Numerical Studies and Performance Evaluation of Proposed Procedure

To assess the effectiveness of the proposed computational procedure and partitioning strategy, a number of dynamic problems of unsymmetric structures have been solved by using this procedure on two CRAY X-MP/4 computer systems at CRAY Research, Inc., Mendota Heights, Minnesota—namely, an X-MP/48 and an X-MP/416 (see appendix D and table II for a summary of the characteristics of these

machines). For each problem, the accuracy and computational time required by the proposed procedure were compared with those of the direct analysis of the (full) structure. Herein, the results are presented for a typical problem of a laminated anisotropic cylindrical panel with an off-center circular cutout. The loading is assumed to be uniformly distributed and normal to the panel surface and to have a step variation in time. The panel is made of graphite-epoxy material. The material and geometric characteristics of the panel are given in figure 3.

A total of 192 mixed elements were used for the spatial discretization of the panel. Biquadratic shape functions were used for approximating each of the generalized displacements, and bilinear shape functions were used for approximating each of the stress resultants (a total of 6144 stress-resultant parameters, 3818 nonzero displacement degrees of freedom, and 3818 nonzero velocity components). The element characteristics are given in reference 22.

### 6.1 Time History Response of the Structure

The panel was divided into four substructures and the proposed procedure was applied to reduce the size of the analysis model to that of the corresponding doubly symmetric structure. Reflection symmetry (and antisymmetry) was assumed with respect to each of the interfaces between the different substructures. These symmetries (and antisymmetries) are typically exhibited by the response of orthotropic panels with a symmetric geometry and symmetric boundary conditions when subjected to symmetric (and antisymmetric) loading.

The temporal integration was performed with the implicit Park three-step method. Galerkin's method (Crank-Nicholson scheme) and the Gear two-step method were used to start the computation (for the first and second time steps, respectively). For the linear case, the critical time step for numerical stability is $\Delta t_{cr} = 0.1194$ $\mu$sec. The time step selected in the present study was 50 $\mu$sec. Both the small displacement (linear) and the large displacement (geometrically nonlinear) elastic responses of the panel were generated for a duration of 3 msec (60 time steps). An energy balance check (ref. 23) was performed at each time step to ensure the accuracy of the solution. At each time step, 3 Newton-Raphson iterations and an average of 20 PCG iterations (per Newton-Raphson iteration) were required to obtain 5 significant digits of accuracy of the response quantities. Solutions obtained by using the proposed strategy were compared with the corresponding solutions obtained by analyzing the full panel (using the same temporal integration scheme, same time step, and same number of Newton-Raphson iterations at each time step).

The time histories of the normal displacement component $w_a$ and the normal velocity component $\dot{w}_a$ at point a, the total complementary strain energy $U^c$, and the total kinetic energy $\overset{\star}{K}$ are shown in figure 4. Point a corresponds to a midside node which exhibited the maximum absolute value for the normal displacement component during the transient analysis. Normalized contour plots for the generalized displacements and velocity components at $t =$ 3.0 msec of both the linear and nonlinear responses are shown in figure 5. Each generalized displacement and velocity component is normalized by its maximum absolute value as given in table III.

### 6.2 Efficiency Gain Obtained by Using the Proposed Procedure

To assess the efficiency gain resulting from the use of the proposed procedure and partitioning strategy, the measured CP times, wall-clock times, and processing rates obtained by using the present computational procedure were compared with those of the direct analysis of the panel (no partitioning). The measured analysis times and processing rates for the first 10 time steps are given in table IV and in figures 6 to 8. The CP times and processing rates on a single CPU were obtained by using the FLOP TRACE (on the X-MP/48) and PERF TRACE (on the X-MP/416) utilities of the CRAY computer. (See ref. 24 and appendix D.) The wall-clock times for two and four CPU's were recorded.

The application of the partitioning strategy outlined in section 3 resulted in reducing the number of nonzero displacement and velocity degrees of freedom from 3818 to 971 and the stress-resultant parameters from 6144 to 1536. The semibandwidth of the global matrices was reduced from 700 to 315.

When a single CPU was used, the measured wall-clock time for the *direct analysis* was 319.7 sec on the X-MP/416. The corresponding wall-clock time for the proposed procedure was 122.6 sec. Because of extensive use of vectorization and chaining in the implementation, the *sustained processing rate* for the direct analysis was 160 MFLOPS (Millions of FLoating point Operations Per Second). The corresponding sustained rate for the proposed procedure was only 119.6 MFLOPS.

The measured CP times and speed or processing rates on a single CPU for the different modules of the proposed strategy are shown in figures 6 and 7. As expected, the majority of the time, 91.3 sec (75 percent of the total time), is expended in the decomposition of the four preconditioning matrices $[\bar{\bar{K}}]$ with

different symmetry/antisymmetry conditions at each Newton-Raphson iteration of each time step. The total time expended in the PCG iterations was 11 sec (9 percent of the total time). As can be seen from figure 7, the processing rates of most of the modules was over 100 MFLOPS. The analysis times for the proposed procedure on two and four CPU's were 66.7 and 36.3 sec, respectively, on the X-MP/416. The speedups gained by multiprocessing are 1.84 and 3.38 on two and four CPU's, respectively.

The total speedup $S_T$ achieved by the proposed procedure is defined as the ratio of the wall-clock time for the direct analysis of the full structure on a single CPU divided by the wall-clock time for the partitioned structure on multiple CPU's. The values of $S_T$ on the X-MP/416 were 2.61, 4.79, and 8.81 for one, two, and four CPU's, respectively.

The corresponding analysis times, speedups, and values of $S_T$ on the X-MP/48 are given in figure 8 and table IV. The reduction in wall-clock times and the increase in speedups on the X-MP/416 (as compared with those on the X-MP/48) are due primarily to the increased number of interleaved memory banks, which results in fewer memory conflicts. It is anticipated that the speedup ratios can be increased by further optimizing the FORTRAN code used in implementing the computational procedure of the partitioning strategy. The sustained processing rate would then be increased to that of the direct analysis implementation.

## 7. Comments on Proposed Computational Procedure

The numerical results presented in the preceding section clearly demonstrate the effectiveness of the proposed partitioning strategy for predicting the nonlinear dynamic response of unsymmetric structures on multiprocessor computers. In particular, the following comments can be made regarding the key elements and the procedure and its key elements:

1. Even though the mixed finite element models used herein have been shown to be equivalent to reduced integration displacement models (ref. 22), the use of mixed (primitive variable) formulation was found to be essential for solving highly unsymmetric problems, with strong coupling between the symmetric and antisymmetric components of the response. *The internal forces (or stress resultants) should only be eliminated after, not before, the application of operator splitting.*

2. The application of operator splitting in conjunction with symmetry transformations allows the restructuring of the discrete equations at each time step to delineate the symmetric and antisymmetric vectors constituting the response, as well as the coupling terms between these vectors.

3. The preconditioned conjugate gradient (PCG) was found to be a highly efficient and stable technique for handling highly unsymmetric problems.

4. The proposed computational procedure can be thought of as generating the dynamic response of an unsymmetric structure, ***using small or large perturbations*** from the response of a simpler structure in which the symmetric/antisymmetric components of the response vector, at any time, are uncoupled.

5. The proposed procedure can also be used for the efficient dynamic analysis of unsymmetric structures on single-processor computers. This is because the uncoupled equations, for the symmetric and antisymmetric response quantities, are the same except for the terms associated with the interface unknowns. (See, for example, eqs. (B26) to (B31).) The efficient generation of the symmetric and antisymmetric response quantities (eqs. (C3), (C6) to (C8), and (C28) to (C31)) can therefore be accomplished by

(a) Single partial decomposition of one set of equations (e.g., the equations associated with $\{\bar{\bar{Y}}\}$ which do not include the symmetry/antisymmetry conditions along the interfaces)

(b) Incorporation of the symmetry/antisymmetry conditions, completing the decomposition, evaluating the right-hand sides, and successively generating the symmetric and antisymmetric response vectors

6. As the number of symmetry transformations increases, the coupling between the symmetric/antisymmetric components of the response vector increases and, therefore, the number of iterations in the PCG technique increases. Consequently, the proposed procedure may not be effective on multiprocessor computers with fine granularity and small local memories (e.g., the hypercubes and the Connection Machine of Thinking Machine, Inc.).

## 8. Concluding Remarks

A computational procedure is presented for nonlinear dynamic analysis on vector multiprocessor computers. The procedure is based on a novel hierarchical partitioning strategy in which the response of an unsymmetric structure at any time instant is approximated by a linear combination of symmetric and antisymmetric response vectors (or modes), each obtained by using only a fraction of the degrees of freedom of the original finite element model.

The analytical formulation is based on a moderate-rotation geometrically nonlinear theory of the structure. A mixed formulation is used in

which the fundamental unknowns consist of the internal forces (or stress resultants), the generalized displacements, and the velocity components of the structure. The spatial discretization is performed by using mixed finite element models with the stress resultants allowed to be discontinuous at interelement boundaries. An implicit, multistep, one-derivative scheme is used for the temporal integration.

The three key elements of the procedure which result in a high degree of concurrency throughout the solution process are (1) mixed (or primitive variable) formulation with independent shape functions for the different fields, (2) operator splitting or restructuring of the governing discrete equations at each time step to delineate the symmetric and antisymmetric vectors constituting the response, and (3) two-level iterative process for generating the response of the structure. The top- and bottom-level iterations (outer and inner iteration loops) are performed by using Newton-Raphson and preconditioned conjugate gradient (PCG) techniques, respectively.

The procedure has been implemented on the CRAY X-MP/4 computers at Cray Research, Inc., Mendota Heights, Minnesota. An assessment is made of the speedup resulting from the use of the proposed procedure. The wall-clock times, central processing times, and processing rates are presented for a typical problem of the dynamic response of a laminated anisotropic cylindrical panel with an off-center circular cutout. The loading is assumed to be uniformly distributed and normal to the panel surface and to have a step variation in time. The use of the foregoing procedure and partitioning strategy reduces the total computational time by nearly an order of magnitude compared with that required by the direct analysis (on a single processor) for the first 10 steps.

NASA Langley Research Center
Hampton, VA 23665-5225
November 14, 1988

## Appendix A

## Governing Discrete Equations of the Structure

In the present study, the temporal integration is performed by using an implicit, multistep, one-derivative scheme. For a constant time step size $\Delta t$, the linear multistep operators have the following form (see refs. 25 and 26):

$$\sum_{l=0}^{m} \alpha_{i-l} \Psi_{i-l} = \Delta t \sum_{l=0}^{m} \beta_{i-l} \left( \frac{d\Psi}{dt} \right)_{i-l} \tag{A1}$$

or

$$\Delta t \beta_i \left( \frac{d\Psi}{dt} \right)_i = \alpha_i \Psi_i + \sum_{l=1}^{m} \left[ \alpha_{i-l} \Psi_{i-l} - \Delta t \beta_{i-l} \left( \frac{d\Psi}{dt} \right)_{i-l} \right] \tag{A2}$$

where $\Psi$ refers to any of the fundamental unknowns; $m$ is the number of steps; and $\alpha$ and $\beta$ are coefficients associated with the various difference operators. The values of these coefficients for the three operators considered in the present study are given in table AI.

Table AI. Coefficients in Multistep Operators

| Coefficient | Galerkin's method | Gear two-step method | Park three-step method |
|---|---|---|---|
| $\alpha_i$ . . . . . | 1 | 1 | 1 |
| $\alpha_{i-1}$ . . . . . | −1 | −4/3 | −1.5 |
| $\alpha_{i-2}$ . . . . . | 0 | 1/3 | 0.6 |
| $\alpha_{i-3}$ . . . . . | 0 | 0 | −0.1 |
| $\beta_i$ . . . . . | 2/3 | 2/3 | 0.6 |
| $\beta_{i-1}$ . . . . . | 1/3 | 0 | 0 |

For the application of the multistep integration schemes, it is convenient to transform the governing equations of the structure (eqs. (1) and (2)) into a system of simultaneous first-order ordinary differential equations. This is accomplished by differentiating the constitutive relations (eqs. (1)) with respect to time. The resulting equations can be written in the form:

$$\frac{d}{dt}([F]\{H\} - \{G(X)\}) = [S]\{V\} \tag{A3}$$

If equation (A2) is used, the governing differential equations (eqs. (2) and (A3)) can be transformed into a system of nonlinear simultaneous algebraic equations in $\{H\}$ and $\{V\}$ at time $i$. Based on an initial estimate for $\{X\}$ and/or $\{V\}$, an iterative Newton-Raphson scheme can be used for the solution of the nonlinear algebraic equations. The iterative process is represented by the following equations for the $r$th iteration cycle:

$$[K]_i^{(r)} \{\Delta\psi\}_i^{(r)} = \{Q\}_i^{(r)} \tag{A4}$$

$$\{\psi\}_i^{(r+1)} = \{\psi\}_i^{(r)} + \{\Delta\psi\}_i^{(r)} \tag{A5}$$

where

$$[K]_i^{(r)} = \begin{bmatrix} -\alpha_i[F] & \Delta t \beta_i \left( [S] + \left[ \frac{\partial G_p}{\partial X_q} \right]_i \right) \\ Symm & \alpha_i[M] + \frac{(\Delta t \beta_i)^2}{\alpha_i} \left[ \frac{\partial N_p}{\partial X_q} \right]_i \end{bmatrix}^{(r)} \tag{A6}$$

$$\{Q\}_i^{(r)} = -\left\{ \begin{matrix} f_H \\ f_V \end{matrix} \right\}_i^{(r)} = \sum_{l=0}^{m} \left( - \begin{bmatrix} -\alpha_{i-l}[F] & \Delta t \beta_{i-l}[S] \\ Symm & \alpha_{i-l}[M] \end{bmatrix} \left\{ \begin{matrix} H \\ V \end{matrix} \right\}_{i-l}^{(r)} \right.$$

$$\left. - \left\{ \begin{matrix} \alpha_{i-l}\{G(X)\}_{i-l} \\ \Delta t \beta_{i-l}\{N(H,X)\}_{i-l} \end{matrix} \right\}^{(r)} + \Delta t \beta_{i-l} \left\{ \begin{matrix} 0 \\ P \end{matrix} \right\}_{i-l} \right) \tag{A7}$$

$$\{\psi\} = \left\{ \begin{matrix} H \\ V \end{matrix} \right\} \tag{A8}$$

If the stress-resultant parameters are eliminated, then equations (A4) can be replaced by the following equations in the velocity components:

$$[K_V]_i^{(r)} \{\Delta V\}_i^{(r)} = \{Q_V\}_i^{(r)} \tag{A9}$$

where

$$[K_V]_i^{(r)} = [K_{VV}] - [K_{HV}]^T [K_{HH}]^{-1} [K_{HV}] \tag{A10}$$

$$\{Q_V\}_i^{(r)} = -\{f_V\}_i^{(r)} + [K_{HV}]^T [K_{HH}]^{-1} \{f_H\}_i^{(r)} \tag{A11}$$

$$[K_{VV}] = \alpha_i [M] + \frac{(\Delta t \beta_i)^2}{\alpha_i} \left[ \frac{\partial N_p}{\partial X_q} \right]_i^{(r)} \tag{A12}$$

$$[K_{HV}] = \Delta t \beta_i \left( [S] + \left[ \frac{\partial G_p}{\partial X_q} \right]_i^{(r)} \right) \tag{A13}$$

$$[K_{HH}] = -\alpha_i [F] \tag{A14}$$

Note that since the stress resultants are allowed to be discontinuous at interelement boundaries, the elimination can be done on the element level (i.e., before assembly).

The nodal displacements $\{X\}_i^{(r+1)}$ at the end of the $r$th iteration cycle, at time $i$, are computed by using the multistep formula:

$$\{X\}_i^{(r+1)} = \Delta t \frac{\beta_i}{\alpha_i} \{V\}_i^{(r+1)} + \frac{1}{\alpha_i} \sum_{l=1}^{m} \left( -\alpha_{i-1} \{X\}_{i-l} + \Delta t \beta_{i-l} \{V\}_{i-l} \right) \tag{A15}$$

The iterative process is continued until convergence. An assessment of the solution accuracy can be made by using an energy balance check at the end of each time step and reducing the time step when the error exceeds a prescribed tolerance. (See ref. 23.)

## Appendix B

## Symmetry Transformations

For the application of symmetry transformations, the structure is first divided into two partitions (or substructures), m = 2. For convenience, each of the two substructures is assumed to have the same number of elements, the same number of nodal displacements, and the same number of nodal velocities. In addition, the interface between the two substructures is assumed to be along the displacement and velocity nodes, and no stress parameters are associated with the interface. As an aid to the visualization of the symmetric and antisymmetric vectors, a symmetrized finite element grid is introduced which has the same symmetry as that of the vectors. The symmetrized grid is constructed on a symmetric domain having the same planform (and/or surface) area as that of the original unsymmetric structure. (See fig. 1.)

The vectors of stress parameters, nodal displacements, nodal velocities, and external loads $\{H\}, \{X\}, \{V\}$, and $\{Q\}$ are partitioned into subvectors $\{H\}_1, \{H\}_2; \{X\}_1, \{X\}_2, \{X\}_3; \{V\}_1, \{V\}_2, \{V\}_3$; and $\{Q\}_1, \{Q\}_2$, $\{Q\}_3$. The subvectors with subscript 1 are associated with one of the substructures, the subvectors with subscript 2 are associated with the other substructure, and the subvectors with subscript 3 are associated with the interface between the two substructures.

The matrices $[F], [S]$, and $[M]$ and the vectors $\{G(X)\}, \{N(H,X)\}$, and $\{Q\}$ used in the discrete equations of the structure (eqs. (A6) and (A7)) are partitioned in submatrix blocks as follows:

$$[F] = \begin{bmatrix} F_{11} & \cdot \\ \cdot & F_{22} \end{bmatrix} \tag{B1}$$

$$[S] = \begin{bmatrix} S_{11} & \cdot & S_{13} \\ \cdot & S_{22} & S_{23} \end{bmatrix} \tag{B2}$$

$$[M] = \begin{bmatrix} M_{11} & \cdot & M_{13} \\ & M_{22} & M_{23} \\ Symm & & M_{33} \end{bmatrix} \tag{B3}$$

$$\{G(X)\} = \begin{Bmatrix} G_1(X_1, X_3) \\ G_2(X_2, X_3) \end{Bmatrix} \tag{B4}$$

$$\{N(H,X)\} = \begin{Bmatrix} N_1(H_1, X_1, X_3) \\ N_2(H_2, X_2, X_3) \\ N_3(H_1, H_2, X_1, X_2, X_3) \end{Bmatrix} \tag{B5}$$

$$\{Q\} = \begin{Bmatrix} Q_1 \\ Q_2 \\ Q_3 \end{Bmatrix} \tag{B6}$$

where a dot in equations (B1) to (B3) refers to a zero submatrix (or subvector). The symmetric and antisymmetric partitions of the vectors $\{H\}, \{X\}, \{V\}$, and $\{Q\}$ are defined as follows:

$$\begin{Bmatrix} H_s \\ H_a \end{Bmatrix} = \begin{bmatrix} \bar{T}_H \\ \tilde{T}_H \end{bmatrix} \begin{Bmatrix} H_1 \\ H_2 \end{Bmatrix} \tag{B7}$$

$$\begin{Bmatrix} X_s \\ X_a \end{Bmatrix} = \begin{bmatrix} \bar{T}_X \\ \tilde{T}_X \end{bmatrix} \begin{Bmatrix} X_1 \\ X_2 \end{Bmatrix} \tag{B8}$$

$$\begin{Bmatrix} V_s \\ V_a \end{Bmatrix} = \begin{bmatrix} \bar{T}_V \\ \tilde{T}_V \end{bmatrix} \begin{Bmatrix} V_1 \\ V_2 \end{Bmatrix} \tag{B9}$$

and

$$\begin{Bmatrix} Q_s \\ Q_a \end{Bmatrix} = \begin{bmatrix} \bar{T}_Q \\ \tilde{T}_Q \end{bmatrix} \begin{Bmatrix} Q_1 \\ Q_2 \end{Bmatrix} \tag{B10}$$

where

$$[\bar{T}_H] = \frac{1}{2}\begin{bmatrix} [I] & [I] \end{bmatrix} \tag{B11}$$

$$[\tilde{T}_H] = \frac{1}{2}\begin{bmatrix} [I] & -[I] \end{bmatrix} \tag{B12}$$

$$[\bar{T}_X] = [\bar{T}_V] = [\bar{T}_Q] = \frac{1}{2}\begin{bmatrix} [I] & [I] \end{bmatrix} \tag{B13}$$

$$[\tilde{T}_X] = [\tilde{T}_V] = [\tilde{T}_Q] = \frac{1}{2}\begin{bmatrix} [I] & -[I] \end{bmatrix} \tag{B14}$$

and the matrix $[I]$ is the identity submatrix. Again, a bar ($^-$) and a tilde ($\tilde{}$) over a vector denote the symmetric and the antisymmetric components of that vector. In equations (B7) to (B10), the subscripts $s$ and $a$ refer to the symmetric and antisymmetric components, respectively. Note that $\{H\}_2, \{X\}_2, \{V\}_2$, and $\{Q\}_2$ account for the change in sign of the antisymmetric components associated with the symmetric response (e.g., transverse shear stress resultants, in-plane displacements, and rotation components in a shell structure, see ref. 27). For symmetric structures subjected to symmetric loading $\{H\}_2 = \{H\}_1, \{X\}_2 = \{X\}_1, \{V\}_2 = \{V\}_1$, and $\{Q\}_2 = \{Q\}_1$.

The following relations follow from equations (B7) to (B14):

$$\begin{Bmatrix} H_1 \\ H_2 \end{Bmatrix} = [T_H] \begin{Bmatrix} H_s \\ H_a \end{Bmatrix} \tag{B15}$$

$$\begin{Bmatrix} X_1 \\ X_2 \\ X_3 \end{Bmatrix} = [T_X] \begin{Bmatrix} X_s \\ X_{3s} \\ X_a \\ X_{3a} \end{Bmatrix} \tag{B16}$$

$$\begin{Bmatrix} V_1 \\ V_2 \\ V_3 \end{Bmatrix} = [T_V] \begin{Bmatrix} V_s \\ V_{3s} \\ V_a \\ V_{3a} \end{Bmatrix} \tag{B17}$$

where

$$[T_H] = \begin{bmatrix} [I] & [I] \\ [I] & -[I] \end{bmatrix} \tag{B18}$$

$$[T_X] = [T_V] = \begin{bmatrix} [I] & \cdot & [I] & \cdot \\ [I] & \cdot & -[I] & \cdot \\ \cdot & [\Gamma_s] & \cdot & [\Gamma_a] \end{bmatrix} \tag{B19}$$

The vectors $\{X_{3s}\}, \{V_{3s}\}$ and $\{X_{3a}\}, \{V_{3a}\}$ refer to the symmetric and antisymmetric components of $\{X\}_3$ and $\{V\}_3$; a dot refers to zero submatrix; $[\Gamma_s]$ and $[\Gamma_a]$ are diagonal submatrices with nonzero (unit) entries corresponding to the symmetric and antisymmetric components of each vector, such that

$$[\Gamma_s] + [\Gamma_a] = [I] \tag{B20}$$

Equations (A4) are now embedded in a single-parameter family of equations of the form:

$$\left[[\bar{K}]_i + \lambda_0[\tilde{K}]_i\right]^{(r)}\{\Delta\psi\}^{(r)} = \{\bar{Q}\}_i^{(r)} + \lambda_0\{\tilde{Q}\}_i^{(r)} \tag{B21}$$

where

$$[\bar{K}]_i^{(r)} = \begin{bmatrix} -\alpha_i[\bar{F}] & \Delta t\beta_i\left([\bar{S}] + \left[\frac{\partial \bar{G}_p}{\partial X_q}\right]_i\right) \\ Symm & \alpha_i[\bar{M}] + \frac{(\Delta t\beta_i)^2}{\alpha_i}\left[\frac{\partial \bar{N}_p}{\partial X_q}\right]_i \end{bmatrix} \tag{B22}$$

$$[\tilde{K}]_i^{(r)} = \begin{bmatrix} -\alpha_i[\tilde{F}] & \Delta t\beta_i\left([\tilde{S}] + \left[\frac{\partial \tilde{G}_p}{\partial X_q}\right]_i\right) \\ Symm & \alpha_i[\tilde{M}] + \frac{(\Delta t\beta_i)^2}{\alpha_i}\left[\frac{\partial \tilde{N}_p}{\partial X_q}\right]_i \end{bmatrix} \tag{B23}$$

$$\{\bar{Q}\}_i^{(r)} = -\left\{\begin{matrix} \bar{f}_H \\ \bar{f}_V \end{matrix}\right\}_i^{(r)} \tag{B24}$$

$$\{\tilde{Q}\}_i^{(r)} = -\left\{\begin{matrix} \tilde{f}_H \\ \tilde{f}_V \end{matrix}\right\}_i^{(r)} \tag{B25}$$

$$[\bar{F}] = \begin{bmatrix} F_{11} + F_{22} & \cdot \\ \cdot & F_{11} + F_{22} \end{bmatrix} \tag{B26}$$

$$[\tilde{F}] = \begin{bmatrix} \cdot & F_{11} - F_{22} \\ F_{11} - F_{22} & \cdot \end{bmatrix} \tag{B27}$$

$$[\bar{S}] = \begin{bmatrix} S_{11} + S_{22} & (S_{13} + S_{23})[\Gamma_s] & \cdot & \cdot \\ \cdot & \cdot & S_{11} + S_{22} & (S_{13} - S_{23})[\Gamma_a] \end{bmatrix} \tag{B28}$$

$$[\tilde{S}] = \begin{bmatrix} \cdot & \cdot & S_{11} - S_{22} & (S_{13} + S_{23})[\Gamma_a] \\ S_{11} - S_{22} & (S_{13} - S_{23})[\Gamma_s] & \cdot & \cdot \end{bmatrix} \tag{B29}$$

$$[\bar{M}] = \begin{bmatrix} M_{11} + M_{22} & (M_{13} + M_{23})[\Gamma_s] & \cdot & \cdot \\ & [\Gamma_s]^T[M_{33}][\Gamma_s] & \cdot & \cdot \\ & & M_{11} + M_{22} & (M_{13} - M_{23})[\Gamma_a] \\ Symm & & & [\Gamma_a]^T[M_{33}][\Gamma_a] \end{bmatrix} \tag{B30}$$

$$[\tilde{M}] = \begin{bmatrix} \cdot & \cdot & M_{11} - M_{22} & (M_{13} + M_{23})[\Gamma_a] \\ \cdot & [\Gamma_s]^T\left([M_{13}]^T - [M_{23}]^T\right)[\Gamma_s] & \cdot & M_{33}[\Gamma_a] \\ Symm & & \cdot & \cdot \end{bmatrix} \tag{B31}$$

$$\{\bar{f}_H\} = \left\{\begin{matrix} \{f_H\}_1 + \{f_H\}_2 \\ \cdot \end{matrix}\right\} \tag{B32}$$

$$\{\tilde{f}_H\} = \begin{Bmatrix} \cdot \\ \{f_H\}_1 - \{f_H\}_2 \end{Bmatrix} \tag{B33}$$

$$\{\bar{f}_V\} = \begin{Bmatrix} \{f_V\}_1 + \{f_V\}_2 \\ [\Gamma_s]^T \{f_V\}_3 \\ \cdot \\ \cdot \end{Bmatrix} \tag{B34}$$

$$\{\tilde{f}_V\} = \begin{Bmatrix} \cdot \\ \cdot \\ \{f_V\}_1 - \{f_V\}_2 \\ [\Gamma_a]^T \{f_V\}_3 \end{Bmatrix} \tag{B35}$$

and $\lambda_0$ is a tracing parameter which identifies all the coupling terms to the symmetric/antisymmetric components of the response vectors. The expressions for $\left[\frac{\partial \tilde{G}_p}{\partial X_q}\right]$, $\left[\frac{\partial \tilde{G}_p}{\partial X_q}\right]$, $\left[\frac{\partial \tilde{N}_p}{\partial X_q}\right]$, and $\left[\frac{\partial \tilde{N}_p}{\partial X_q}\right]$ are similar to those of $[\bar{S}], [\tilde{S}], [\bar{M}]$, and $[\tilde{M}]$, respectively.

The following comments can be made in connection with the symmetry transformations:

1. When $\lambda_0 = 1$, equations (B21) are equivalent to equations (A4). The case $\lambda_0 = 0$ corresponds to the uncoupled equations associated with the symmetric/antisymmetric components of the response vectors $\{\Delta H\}_i^{(r)}$ and $\{\Delta V\}_i^{(r)}$.

2. The presence of nonzero terms in the matrices with a tilde (˜) signifies the coupling between the symmetric and antisymmetric modes constituting the unsymmetric response. For a symmetric structure with identical substructures, the matrices $[\tilde{F}], [\tilde{S}]$, and $[\tilde{M}]$ are zero, and the equations associated with the symmetric and antisymmetric partitions of the response vectors are uncoupled.

3. For $\lambda_0 = 0$, the equations associated with the symmetric and antisymmetric response quantities are identical except for the terms associated with the interface unknowns $\{\Delta V\}_{3s}$ and $\{\Delta V\}_{3a}$. Therefore, only one set of these equations was considered, and the symmetry/antisymmetry conditions were applied at the interfaces.

4. The symmetry transformations can be applied in a recursive manner to effect further reduction in the size of the partitions (or substructures). To apply the second symmetry transformation (m = 4), each of the response vectors $\{H\}_s, \{H\}_a, \{V\}_s, \{V\}_a, \{X\}_s$, and $\{X\}_a$ is decomposed into symmetric/antisymmetric components (see fig. 2) and the associated matrices in equations (B21), $[\bar{K}]$ and $[\tilde{K}]$, are now decomposed into $[\bar{\bar{K}}], [\tilde{\bar{K}}], [\bar{\tilde{K}}]$, and $[\tilde{\tilde{K}}]$. Also, the right-hand side vectors $\{\bar{Q}\}$ and $\{\tilde{Q}\}$ are decomposed into $\{\bar{\bar{Q}}\}, \{\tilde{\bar{Q}}\}, \{\bar{\tilde{Q}}\}$, and $\{\tilde{\tilde{Q}}\}$.

## Appendix C

## Application of Preconditioned Conjugate Gradient (PCG) Technique

For the case m = 4, the solution of the linear algebraic equations associated with each iteration cycle of the Newton-Raphson technique (eqs. (8)), using the preconditioned conjugate gradient technique, can be divided into four major steps which are outlined subsequently. For convenience, equations (8) are cast in the following form (using a single tracing parameter $\lambda$):

$$\left[[\bar{\bar{K}}]+\lambda([\tilde{\tilde{K}}]+[\bar{\tilde{K}}]+[\tilde{\bar{K}}])\right]\{\Delta\psi\} = \{\bar{\bar{Q}}\}+\lambda(\{\tilde{\tilde{Q}}\}+\{\bar{\tilde{Q}}\}+\{\tilde{\bar{Q}}\}) \quad \text{(C1)}$$

The solution is sought for $\lambda = 1$. The solution vector in each iteration can be decomposed into four symmetric/antisymmetric components as follows:

$$\{\Delta\psi\} = \{\Delta\bar{\bar{\psi}}\}+\{\Delta\tilde{\tilde{\psi}}\}+\{\Delta\bar{\tilde{\psi}}\}+\{\Delta\tilde{\bar{\psi}}\} \quad \text{(C2)}$$

The four major steps of the solution are

Step 1—Initialization:

1. Obtain an initial estimate $\{\Delta\psi\}_0$ of $\{\Delta\bar{\bar{\psi}}\}$ by solving the equations:

$$[\bar{\bar{K}}]\{\Delta\psi\}_0 = \{\bar{\bar{Q}}\} \quad \text{(C3)}$$

Note that $\{\Delta\psi\}_0$ is doubly symmetric; therefore,

$$\{\Delta\bar{\bar{\psi}}\}_0 = \{\Delta\psi\}_0 \quad \text{(C4)}$$

and

$$\{\Delta\tilde{\tilde{\psi}}\}_0 = \{\Delta\bar{\tilde{\psi}}\}_0 = \{\Delta\tilde{\bar{\psi}}\}_0 = 0 \quad \text{(C5)}$$

2. Obtain the symmetric/antisymmetric components of the preconditioned residuals by solving the following three equations:

$$[\bar{\bar{K}}]\{\tilde{\tilde{Y}}\}_0 = \{\tilde{\tilde{Q}}\}-[\tilde{\tilde{K}}]\{\Delta\bar{\bar{\psi}}\}_0 = \{\tilde{\tilde{R}}\}_0 \quad \text{(C6)}$$

$$[\bar{\tilde{K}}]\{\bar{\tilde{Y}}\}_0 = \{\bar{\tilde{Q}}\}-[\bar{\tilde{K}}]\{\Delta\bar{\bar{\psi}}\}_0 = \{\bar{\tilde{R}}\}_0 \quad \text{(C7)}$$

$$[\tilde{\bar{K}}]\{\tilde{\bar{Y}}\}_0 = \{\tilde{\bar{Q}}\}-[\tilde{\bar{K}}]\{\Delta\bar{\bar{\psi}}\}_0 = \{\tilde{\bar{R}}\}_0 \quad \text{(C8)}$$

and

$$\{\bar{\bar{Y}}\}_0 = \{\bar{\bar{R}}\}_0 = 0) \quad \text{(C9)}$$

The vectors $\{R\}_0$ refer to the initial residual vector. Note that different symmetry/antisymmetry conditions are incorporated into the matrices $[\bar{\bar{K}}]$ on the left-hand sides of equations (C6) to (C8).

3. Initialize the symmetric/antisymmetric components of the conjugate search direction vectors:

$$\{\bar{\bar{Z}}\}_0 = \{\bar{\bar{Y}}\}_0 = 0 \qquad \{\tilde{\tilde{Z}}\}_0 = \{\tilde{\tilde{Y}}\}_0 \quad \text{(C10)}$$

$$\{\bar{\tilde{Z}}\}_0 = \{\bar{\tilde{Y}}\}_0 \qquad \{\tilde{\bar{Z}}\}_0 = \{\tilde{\bar{Y}}\}_0 \quad \text{(C11)}$$

Step 2—Line search and updating of solution and residual:

For $j = 0$, step $j$ by 1 until convergence and do the following:

4. Compute the step length $\bar{\alpha}_j$ along the search direction:

$$\bar{\alpha}_j = \frac{a_j}{b_j} \quad \text{(C12)}$$

where

$$a_j = \{\bar{\bar{Y}}\}_j^T\{\bar{\bar{R}}\}_j+\{\tilde{\tilde{Y}}\}_j^T\{\tilde{\tilde{R}}\}_j+\{\bar{\tilde{Y}}\}_j^T\{\bar{\tilde{R}}\}_j+\{\tilde{\bar{Y}}\}_j^T\{\tilde{\bar{R}}\}_j \quad \text{(C13)}$$

$$b_j = \{\bar{\bar{Z}}\}_j^T\{\bar{\bar{z}}\}_j+\{\tilde{\tilde{Z}}\}_j^T\{\tilde{\tilde{z}}\}_j+\{\bar{\tilde{Z}}\}_j^T\{\bar{\tilde{z}}\}_j+\{\tilde{\bar{Z}}\}_j^T\{\tilde{\bar{z}}\}_j \quad \text{(C14)}$$

$$\{\bar{\bar{z}}\}_j = [\bar{\bar{K}}]\{\bar{\bar{Z}}\}_j+[\tilde{\tilde{K}}]\{\tilde{\tilde{Z}}\}_j+[\bar{\tilde{K}}]\{\bar{\tilde{Z}}\}_j+[\tilde{\bar{K}}]\{\tilde{\bar{Z}}\}_j \quad \text{(C15)}$$

$$\{\tilde{\tilde{z}}\}_j = [\bar{\bar{K}}]\{\tilde{\tilde{Z}}\}_j+[\tilde{\tilde{K}}]\{\bar{\bar{Z}}\}_j+[\bar{\tilde{K}}]\{\tilde{\bar{Z}}\}_j+[\tilde{\bar{K}}]\{\bar{\tilde{Z}}\}_j \quad \text{(C16)}$$

$$\{\bar{\tilde{z}}\}_j = [\bar{\bar{K}}]\{\bar{\tilde{Z}}\}_j+[\tilde{\tilde{K}}]\{\tilde{\bar{Z}}\}_j+[\bar{\tilde{K}}]\{\bar{\bar{Z}}\}_j+[\tilde{\bar{K}}]\{\tilde{\tilde{Z}}\}_j \quad \text{(C17)}$$

$$\{\tilde{\bar{z}}\}_j = [\bar{\bar{K}}]\{\tilde{\bar{Z}}\}_j+[\tilde{\tilde{K}}]\{\bar{\tilde{Z}}\}_j+[\bar{\tilde{K}}]\{\tilde{\tilde{Z}}\}_j+[\tilde{\bar{K}}]\{\bar{\bar{Z}}\}_j \quad \text{(C18)}$$

5. Update the symmetric/antisymmetric components of the stress-resultants and velocity increments:

$$\{\Delta\bar{\bar{\psi}}\}_{j+1} = \{\Delta\bar{\bar{\psi}}\}_j+\bar{\alpha}_j\{\bar{\bar{Z}}\}_j \quad \text{(C19)}$$

$$\{\Delta\tilde{\bar{\psi}}\}_{j+1} = \{\Delta\tilde{\bar{\psi}}\}_j+\bar{\alpha}_j\{\tilde{\bar{Z}}\}_j \quad \text{(C20)}$$

$$\{\Delta\bar{\tilde{\psi}}\}_{j+1} = \{\Delta\bar{\tilde{\psi}}\}_j + \bar{\alpha}_j\{\bar{\tilde{Z}}\}_j \quad \text{(C21)}$$

$$\{\Delta\tilde{\tilde{\psi}}\}_{j+1} = \{\Delta\tilde{\tilde{\psi}}\}_j + \bar{\alpha}_j\{\tilde{\tilde{Z}}\}_j \quad \text{(C22)}$$

6. Compute and update the symmetric/antisymmetric components of the new residual vector using the equations:

$$\{\bar{\tilde{R}}\}_{j+1} = -\bar{\alpha}_j\{\bar{\tilde{z}}\}_j + \{\bar{\tilde{R}}\}_j \quad \text{(C23)}$$

$$\{\tilde{\tilde{R}}\}_{j+1} = -\bar{\alpha}_j\{\tilde{\tilde{z}}\}_j + \{\tilde{\tilde{R}}\}_j \quad \text{(C24)}$$

$$\{\bar{\tilde{R}}\}_{j+1} = -\bar{\alpha}_j\{\tilde{\bar{z}}\}_j + \{\bar{\tilde{R}}\}_j \quad \text{(C25)}$$

$$\{\tilde{\bar{R}}\}_{j+1} = -\bar{\alpha}_j\{\tilde{\bar{z}}\}_j + \{\tilde{\bar{R}}\}_j \quad \text{(C26)}$$

Step 3—Convergence check:

7. If

$$|R|_{j+1} \leq \varepsilon|R|_0 \quad \text{(C27)}$$

where $|R|$ is the Euclidean norm of the residual vector and $\varepsilon$ is a prescribed tolerance, then stop, otherwise continue.

Step 4—Computation of new search direction vector:

8. Solve for the symmetric/antisymmetric components of the preconditioned residual vector

$$[\bar{\tilde{K}}]\{\bar{\tilde{Y}}\}_{j+1} = \{\bar{\tilde{R}}\}_{j+1} \quad \text{(C28)}$$

$$[\bar{\tilde{K}}]\{\tilde{\tilde{Y}}\}_{j+1} = \{\tilde{\tilde{R}}\}_{j+1} \quad \text{(C29)}$$

$$[\bar{\tilde{K}}]\{\bar{\tilde{Y}}\}_{j+1} = \{\bar{\tilde{R}}\}_{j+1} \quad \text{(C30)}$$

$$[\bar{\tilde{K}}]\{\tilde{\bar{Y}}\}_{j+1} = \{\tilde{\bar{R}}\}_{j+1} \quad \text{(C31)}$$

9. Compute the orthogonalization coefficient $\bar{\beta}_{j+1}$ using

$$\bar{\beta}_{j+1} = a_{j+1}/a_j \quad \text{(C32)}$$

where the $a$'s are defined in equations (C13).

10. Update the symmetric/antisymmetric components of the conjugate search direction vectors

$$\{\bar{\tilde{Z}}\}_{j+1} = \bar{\beta}_{j+1}\{\bar{\tilde{Z}}\}_j + \{\bar{\tilde{Y}}\}_{j+1} \quad \text{(C33)}$$

$$\{\tilde{\tilde{Z}}\}_{j+1} = \bar{\beta}_{j+1}\{\tilde{\tilde{Z}}\}_j + \{\tilde{\tilde{Y}}\}_{j+1} \quad \text{(C34)}$$

$$\{\bar{\tilde{Z}}\}_{j+1} = \bar{\beta}_{j+1}\{\bar{\tilde{Z}}\}_j + \{\bar{\tilde{Y}}\}_{j+1} \quad \text{(C35)}$$

$$\{\tilde{\bar{Z}}\}_{j+1} = \bar{\beta}_{j+1}\{\tilde{\bar{Z}}\}_j + \{\tilde{\bar{Y}}\}_{j+1} \quad \text{(C36)}$$

## Appendix D

## Summary of Major Features of CRAY X-MP Computers

The CRAY X-MP computer system is a multiprocessor vector machine with shared central memory. The two models used in the present study are the CRAY X-MP/48 and X-MP/416 computers (serial numbers 231 and 218) at Cray Research, Inc., Mendota Heights, Minnesota. Each one of the two models has four CPU's and an ECL bipolar central memory. A summary of the hardware and software characteristics of the two computers is given in table II.

*Each of the CPU's* has the following features:

8.5 nsec clock period
14 functional units
Scalar and vector instructions
Four parallel memory ports connected to the central memory: two for vector and scalar fetches, one for result store, and one for independent input/output operations.

The estimated peak performance of each CPU is 210 MFLOPS. This can only be achieved by using the chaining facility of the CRAY, that is, by overlapping the vector multiply, add, and memory access operations.

*The central memory* has a capacity of 8 Mwords on the X-MP/48 model and 16 Mwords on the X-MP/416 model. The memory is organized into 32 and 64 interleaved banks on the X-MP/48 and the X-MP/416 models.

The two facilities for multiple CPU utilization on the CRAY X-MP system are *macrotasking* and *microtasking*. (See ref. 28.) Macrotasking is done on the FORTRAN subroutine level. User interaction with the macrotasking environment is done via calls to the macrotasking library. Microtasking is done via compiler directives. The granularity of microtasking is finer than that of macrotasking (i.e., down to the outer do-loop level). The overhead associated with microtasking is considerably less than that involved in macrotasking.

A number of *performance monitors* are available on the CRAY X-MP system. The two used in the present study are FLOP TRACE on the X-MP/48 and PERF TRACE on the X-MP/416. (See ref. 24.) Each of the two monitors produces a table showing the subroutine name, the number of times it was called, the execution time, the average time per call, the percentage of total program time spent in the subroutine, the accumulated percentage of total program execution times for subroutines up to the current one, the number of additions, multiplications, and reciprocals performed by the subroutine, the total floating point operations, the ratio of memory references to floating point operations, the memory reference rate, and the processing rate (in MFLOPS). The table is sorted in decreasing percentage, so that the most important routines are at the top of the list. The same statistics are displayed for the program as a whole.

Although these utilities are very useful in identifying the time consuming subroutines and the candidate routines for macrotasking, they are used with one CPU only. To estimate the speedup resulting from multiprocessing, the only facility currently available is measuring the wall-clock time.

## References


1. Noor, Ahmed K.; and Atluri, Satya N.: Advances and Trends in Computational Structural Mechanics. *AIAA J.*, vol. 25, no. 7, July 1987, pp. 977–995.
2. Schwartz, Jacob: *A Taxonomic Table of Parallel Computers, Based on 55 Designs.* Ultracomput. Note No. 69, Courant Inst. of Mathematical Sciences, New York Univ., Nov. 1983.
3. Dongarra, Jack J.; and Duff, Iain S.: *Advanced Architecture Computers.* Tech. Memo. No. 57 (Revision 1), Mathematics & Computer Science Div., Argonne National Lab., Jan. 19, 1987.
4. Hwang, Kai: Advanced Parallel Processing With Supercomputer Architectures. *Proc. IEEE,* vol. 75, no. 10, Oct. 1987, pp. 1348–1379.
5. McBryan, Oliver A.: State-of-the-Art in Highly Parallel Computer Systems. *Parallel Computations and Their Impact on Mechanics,* Ahmed K. Noor, ed., AMD-Vol. 86, American Soc. of Mechanical Engineers, c.1987, pp. 31–47.
6. Schendel, U. (B. W. Conolly, transl.): *Introduction to Numerical Methods for Parallel Computers.* John Wiley & Sons, c.1984.
7. Dongarra, J. J.; and Sorensen, D. C.: Linear Algebra on High-Performance Computers. *Parallel Computing 85,* M. Feilmeier, G. Joubert, and U. Schendel, eds., Elsevier Science Publ., 1986, pp. 3–32.
8. Adams, L.: Reordering Computations for Parallel Execution. *Commun. Appl. Numer. Methods,* vol. 2, no. 3, May–June 1986, pp. 263–271.
9. McBryan, Oliver; and Van de Velde, Eric F.: Matrix and Vector Operations on Hypercube Parallel Processors. *Parallel Comput.,* vol. 5, nos. 1 and 2, July 1987, pp. 117–125.
10. Ortega, James M.: *Introduction to Parallel and Vector Solution of Linear Systems.* Plenum Press, c.1988.
11. Adams, Loyce M.; and Voigt, Robert G.: A Methodology for Exploiting Parallelism. *High-Speed Computation,* J. S. Kowalik, ed., Springer-Verlag, c.1984, pp. 373–392.
12. Carey, Graham F.: Parallelism in Finite Element Modelling. *Commun. Appl. Numer. Methods,* vol. 2, no. 3, May–June 1986, pp. 281–287.
13. Farhat, C. H.; Felippa, C. A.; and Park, K. C.: Implementation Aspects of Concurrent Finite Element Computations. *Parallel Computations and Their Impact on Mechanics,* Ahmed K. Noor, ed., AMD-Vol. 86, American Soc. of Mechanical Engineers, c.1987, pp. 301–315.
14. Flower, J.; Otto, S.; and Salama, M.: Optimal Mapping of Irregular Finite Element Domains to Parallel Processors. *Parallel Computations and Their Impact on Mechanics,* Ahmed K. Noor, ed., AMD-Vol. 86, American Soc. of Mechanical Engineers, c.1987, pp. 239–250.
15. Novozhilov, V. V.: *Theory of Elasticity.* Israel Program for Scientific Translations (Jerusalem), 1961.
16. Noor, Ahmed K.; and Peters, Jeanne M.: Model-Size Reduction for the Non-Linear Dynamic Analysis of Quasi-Symmetric Structures. *Eng. Comput.,* vol. 4, no. 3, Sept. 1987, pp. 178–189.
17. Dongarra, J. J.; Bunch, J. R.; Moler, C. B.; and Stewart, G. W.: *LINPACK User's Guide.* SIAM, 1979.
18. Dongarra, Jack J.: *Performance of Various Computers Using Standard Linear Equations Software in a Fortran Environment.* Tech. Memo. No. 23, Mathematics & Computer Science Div., Argonne National Lab., Apr. 3, 1987.
19. Booth, Mike; and Misegades, Kent: Microtasking: A New Way To Harness Multiprocessors. *CRAY CHANNELS,* vol. 8, no. 2, Summer 1986, pp. 24–27.
20. Misegades, K.; Krause, L.; and Booth, M.: Microtasking of Fluid Mechanics Codes on the CRAY X-MP. *Applications of Parallel Processing in Fluid Mechanics,* Oktay Baysal, ed., FED-Vol. 47, American Soc. of Mechanical Engineers, c.1987, pp. 19–25.
21. Seager, M. K.: Overhead Considerations for Parallelizing Conjugate Gradient. *Commun. Appl. Numer. Methods,* vol. 2, no. 3, May–June 1986, pp. 273–279.
22. Noor, Ahmed K.; and Andersen, C. M.: Mixed Models and Reduced/Selective Integration Displacement Models for Nonlinear Shell Analysis. *Int. J. Numer. Methods Eng.,* vol. 18, no. 10, Oct. 1982, pp. 1429–1454.
23. Belytschko, Ted: An Overview of Semidiscretization and Time Integration Procedures. *Computational Methods for Transient Analysis,* Ted Belytschko and Thomas J. R. Hughes, eds., Elsevier Science Publ. Co., Inc., 1983, pp. 1–65.
24. Larson, John: CRAY X-MP Hardware Performance Monitor. *CRAY CHANNELS,* vol. 7, no. 4, Winter 1986, pp. 18–19.
25. Felippa, C. A.; and Park, K. C.: Computational Aspects of Time Integration Procedures in Structural Dynamics, Part I: Implementation. *Trans. ASME, J. Appl. Mech.,* vol. 45, no. 3, Sept. 1978, pp. 595–602.
26. Van der Houwen, P. J.: *Construction of Integration Formulas for Initial Value Problems.* North-Holland Publ. Co., 1977.
27. Noor, Ahmed K.; and Camin, Robert A.: Symmetry Considerations for Anisotropic Shells. *Comput. Methods Appl. Mech. & Eng.,* vol. 9, no. 3, Nov.–Dec. 1976, pp. 317–335.
28. *Multitasking User Guide.* SN-0222, Cray Research, Inc., Mar. 1986.

Table I. Flowchart of Computational Procedure

Preprocessing Phase

1. Input problem and model data
2. Generate the linear modified elemental arrays (see appendix B)

Solution Phase

3. *Begin time step loop*
4. *Begin Newton-Raphson iteration loop*
5. Predict velocity components, stress resultants, and generalized displacements
6. Generate nonlinear modified elemental arrays on the left-hand side of the equations (see appendix B)
7. Eliminate stress resultants from elemental equations and assemble the left-hand side for the reduced-size model (see eqs. (A9) to (A14))
8. Evaluate right-hand side elemental arrays and assemble them (see eqs. (A7) and (A11))
9. *Begin PCG iteration loop* (see appendix C)
10. Decompose the preconditioning matrices associated with different symmetry/antisymmetry conditions (eqs. (C3), (C6), (C7), and (C8))
11. Calculate the symmetric/antisymmetric components of the residual vector, the preconditioned residuals, step length, orthogonalization coefficient, conjugate search direction, and update the response vectors (tasks numbers 2 through 6 and 8 through 10, appendix C)
12. Check convergence of PCG, if satisfied continue, otherwise go to step 11
13. Check convergence of Newton-Raphson iterations, if satisfied continue, otherwise go to step 6
14. Check if $t = t_{\max}$ then stop, otherwise set $t = t + \Delta t$ and go to step 4

Table II. Characteristics of CRAY X-MP/4 Computer Systems Used in Present Study

| Characteristics | X-MP/48 | X-MP/416 |
|---|---|---|
| Number of CPU's | 4 | 4 |
| Clock cycle, nsec | 8.5 | 8.5 |
| Memory | 8 Mwords[a] (32 banks) central memory | 16 Mwords[a] (64 banks) central memory |
| Storage size | 32 Mwords SSD[b] | 512 Mwords SSD[b] |
| Operating system | COS 1.16 BF2 | UNICOS 3.0.8 |
| Compiler | CFT version 1.15 BF2 | CFT version 1.15 BF2 |
| Performance monitor (on one CPU) | FLOP TRACE | PERF TRACE |

[a]1 Mword $\equiv$ 1 048 576 words (each word is 64 bits).

[b]The SSD (solid-state storage device) functions as a very high speed secondary memory and is treated by the operating system and the user as another disk drive.

Table III. Maximum Absolute Values of Generalized Displacements and Velocity Components, $\{X\}$ and $\{V\}$, at $t = 3.0$ msec

[Laminated anisotropic composite panel with an off-center circular cutout subjected to uniform normal loading $p_o = -50\,000$ Pa (see figs. 3 and 5)]

| | Linear | Nonlinear |
|---|---|---|
| Generalized displacements: | | |
| $\frac{w}{h}$ | 0.2940 | 1.007 |
| $10 \times \frac{u_1}{h}$ | 0.1945 | 0.3634 |
| $10 \times \frac{u_2}{h}$ | 0.7922 | 1.654 |
| $10^2 \times \phi_1$ | 0.9364 | 1.825 |
| $10 \times \phi_2$ | 0.1862 | 0.5595 |
| Velocity components: | | |
| $10^{-4} \times \frac{\dot{w}}{h}$ | 0.2554 | 0.1775 |
| $10^{-2} \times \frac{\dot{u}_1}{h}$ | 0.6049 | 0.2036 |
| $10^{-3} \times \frac{\dot{u}_2}{h}$ | 0.2848 | 0.1237 |
| $10^{-2} \times \dot{\phi}_1$ | 0.8394 | 0.4421 |
| $10^{-3} \times \dot{\phi}_2$ | 0.1482 | 0.1708 |

Table IV. Performance Evaluation of Proposed Strategy on CRAY X-MP/4 Computers

[Laminated anisotropic composite panel with off-center circular cutout subjected to uniform normal loading $p_o = -50\,000$ Pa (see figs. 3 and 5)]

| | X-MP/48 COS 1.16 BF2 operating system, CFT compiler version 1.15 BF2 | | X-MP/416 UNICOS 3.0.8 operating system, CFT compiler version 1.15 BF2 | |
|---|---|---|---|---|
| | Full structure | Partitioned structure | Full structure | Partitioned structure |
| Wall-clock time for first 10 time steps, sec . . . . . | 339 | 123.1 (1 CPU)<br>68.8 (2 CPU's)<br>41.7 (4 CPU's) | 319.7 | 122.6 (1 CPU)<br>66.7 (2 CPU's)<br>36.3 (4 CPU's) |
| Sustained speed on one CPU, MFLOPS . . . . . | 152.1 | 119.1 | 160 | 119.6 |
| Speedup due to multiprocessing . . . . . | | 1.0 (1 CPU)<br>1.79 (2 CPU's)<br>2.95 (4 CPU's) | | 1.0 (1 CPU)<br>1.84 (2 CPU's)<br>3.38 (4 CPU's) |
| Total speedup, $S_T$, achieved by proposed procedure . . . . . | 1.0 | 2.75 (1 CPU)<br>4.93 (2 CPU's)<br>8.13 (4 CPU's) | 1.0 | 2.61 (1 CPU)<br>4.79 (2 CPU's)<br>8.81 (4 CPU's) |

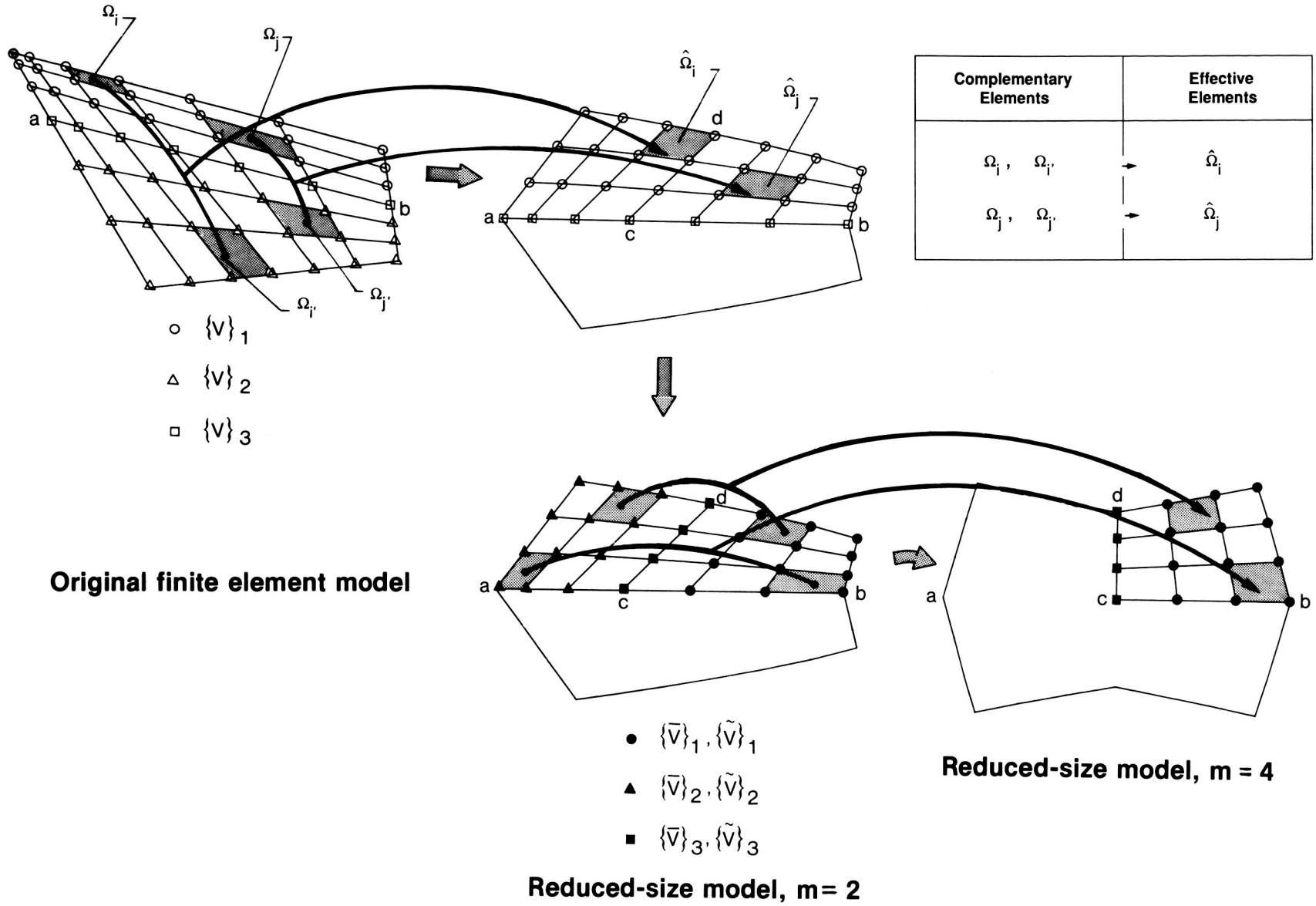


Figure 1. Original finite element model and reduced-size models (substructures).

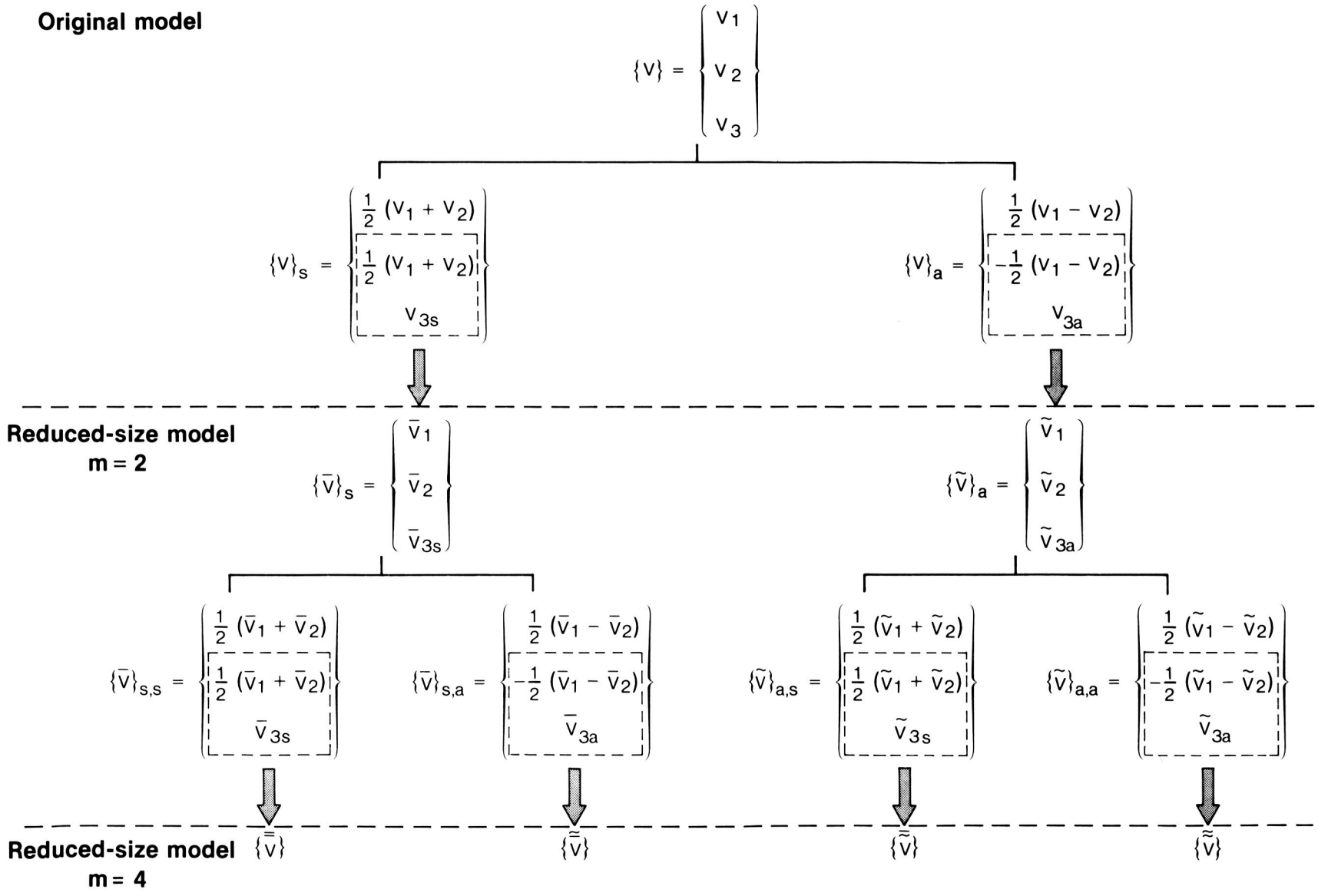


Figure 2. Unknown displacements in original and reduced-size models (substructures).

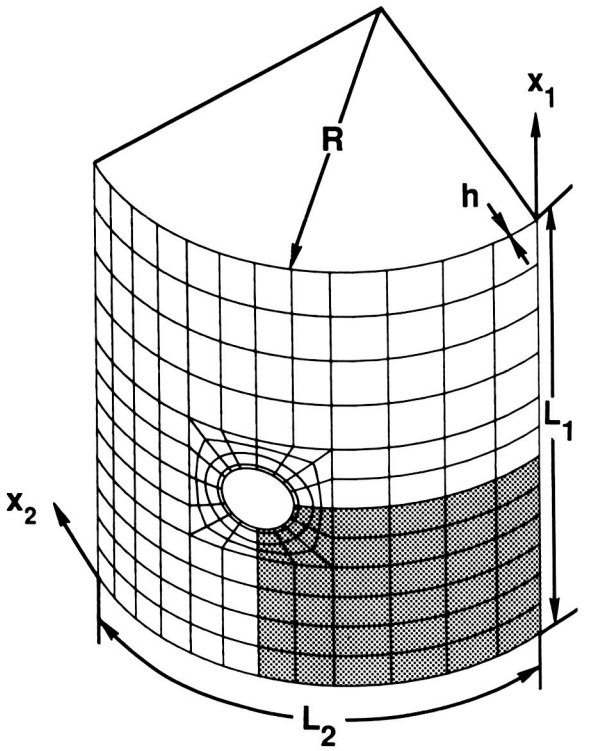


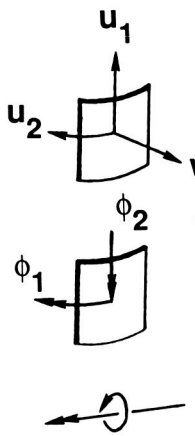


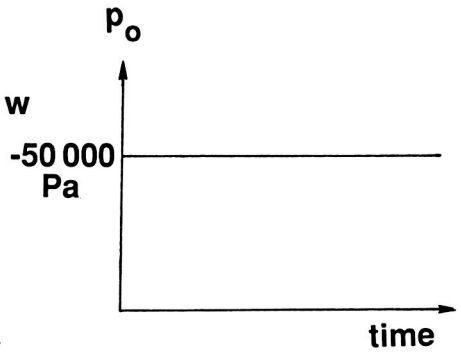


$L_1 = L_2 = 0.3556$ m
$R = 0.381$ m
$h = 2.276$ mm
Hole radius = 0.0254 m
Hole center at 0.1524 = 0.2032 m

$E_L = 131$ GPa
$E_T = 13.03$ GPa
$G_{LT} = 6.412$ GPa
$G_{TT} = 5.102$ GPa
$\nu_{LT} = 0.392$
$\rho = 1522.4$ kg/m$^3$
Fiber orientation:
$[\pm 45/90/0_2/90/\mp 45]_s$

**Boundary conditions:**

At $x_1 = 0, L_1$:
$u_1 = u_2 = w = \phi_1 = \phi_2 = 0$

At $x_2 = 0, L_2$:
$w = \phi_1 = 0$

**Initial conditions:**

At t = 0:

$u_1 = u_2 = w = \phi_1 = \phi_2 = 0$
$\dot{u}_1 = \dot{u}_2 = \dot{w} = \dot{\phi}_1 = \dot{\phi}_2 = 0$

Everywhere

Figure 3. Laminated anisotropic composite panel with off-center circular cutout used in present study.

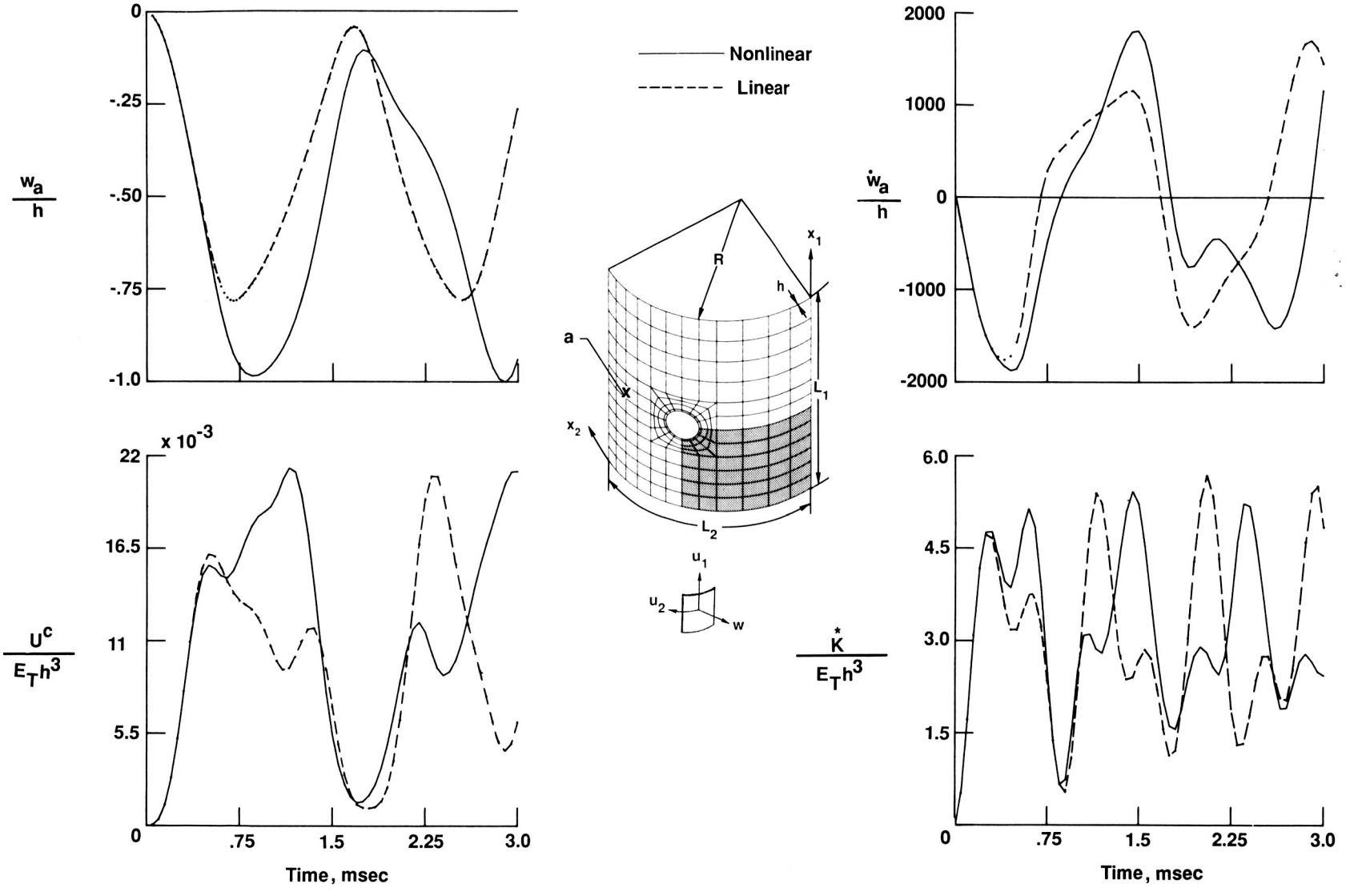


Figure 4. Linear and nonlinear dynamic responses of laminated anisotropic composite panel with off-center circular cutout subjected to uniform normal loading $p_o = -50\,000$ Pa (see fig. 3).

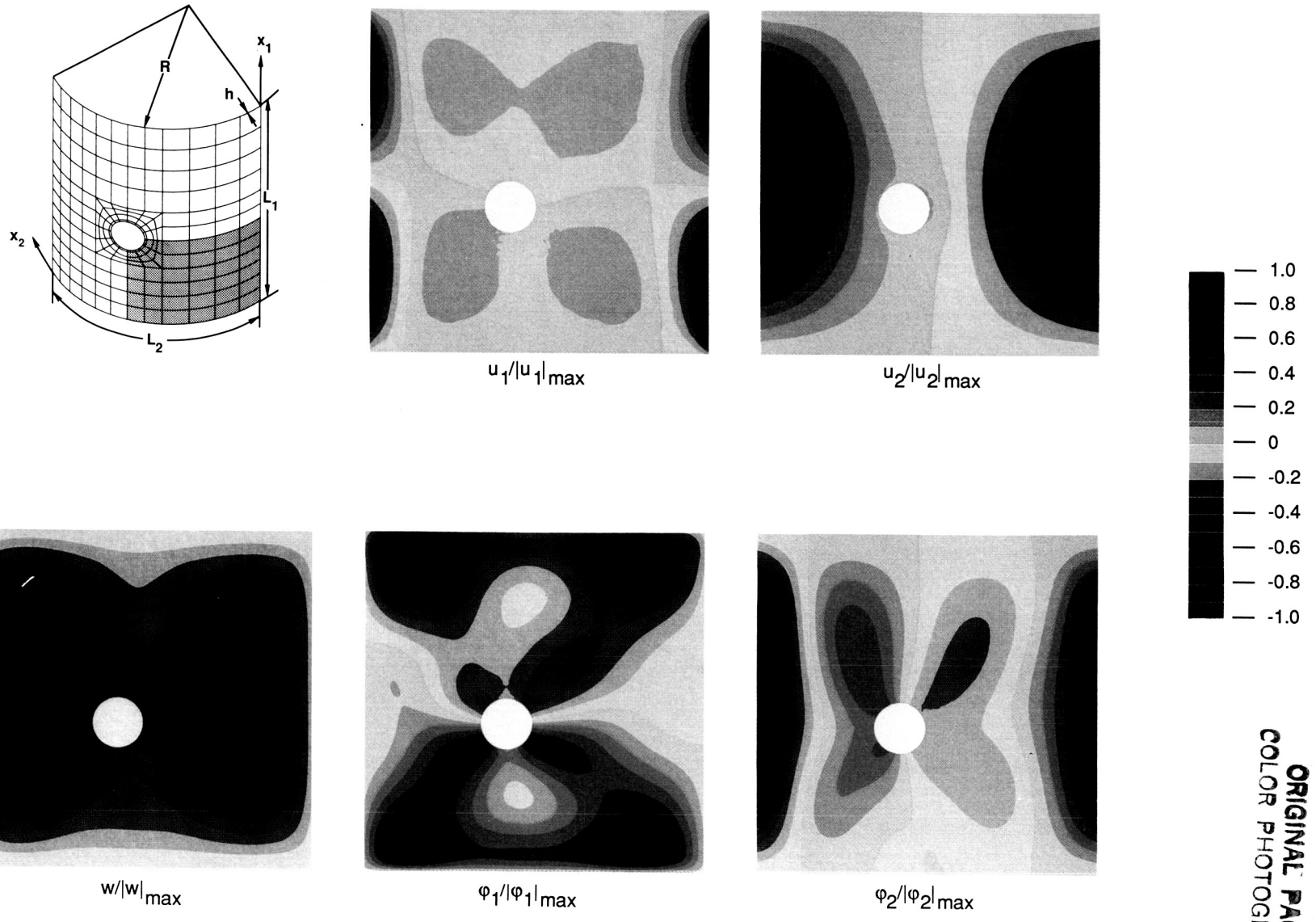


(a) Linear generalized displacements.

Figure 5. Normalized contour plots for generalized displacements and velocity components at $t = 3.0$ msec. Laminated anisotropic composite panel with off-center circular cutout subjected to uniform normal loading $p_o = -50\,000$ Pa (see fig. 3).

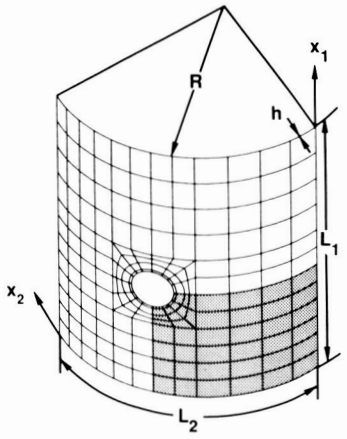


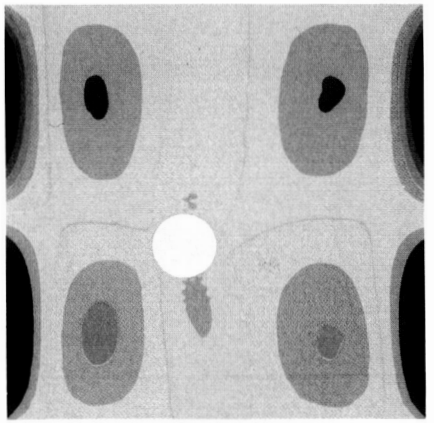

$u_1/|u_1|_{max}$

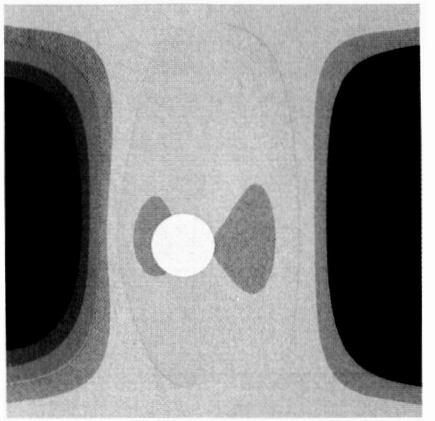

$u_2/|u_2|_{max}$

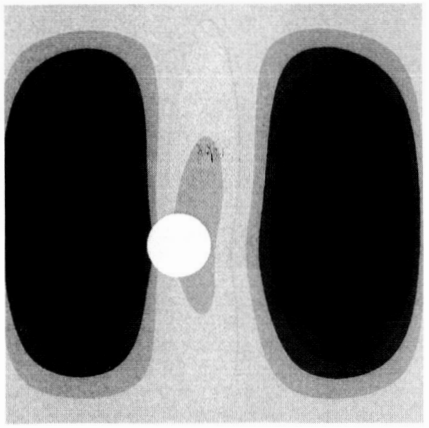

$w/|w|_{max}$

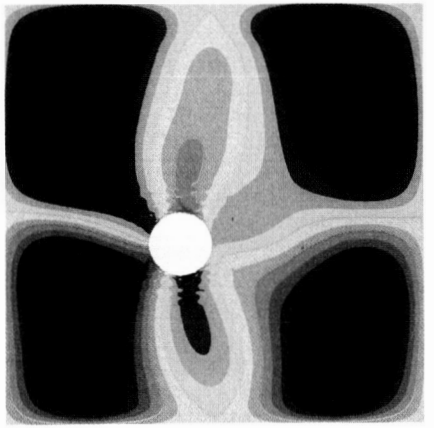

$\varphi_1/|\varphi_1|_{max}$

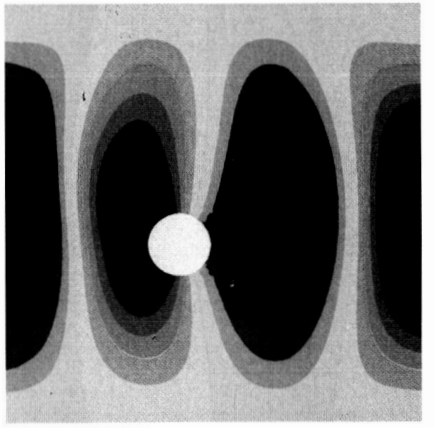

$\varphi_2/|\varphi_2|_{max}$

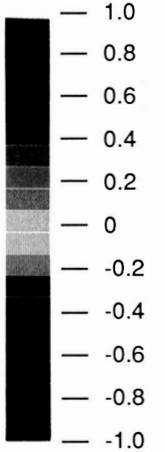




(b) Nonlinear generalized displacements.

Figure 5. Continued.

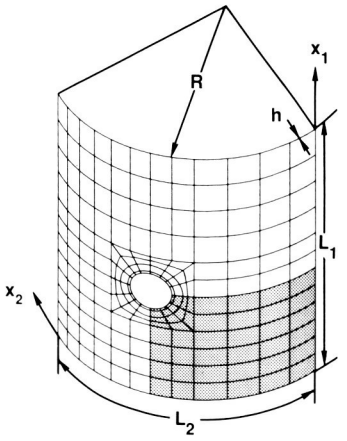


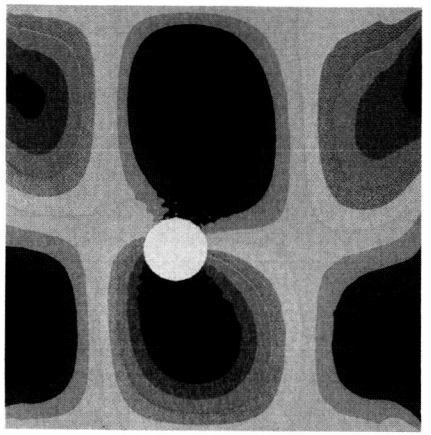

$\dot{u}_1/|\dot{u}_1|_{max}$

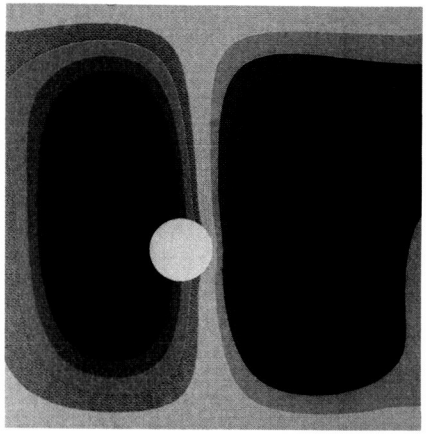

$\dot{u}_2/|\dot{u}_2|_{max}$

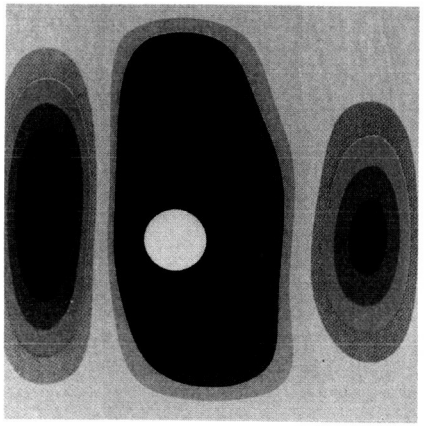

$\dot{w}/|\dot{w}|_{max}$

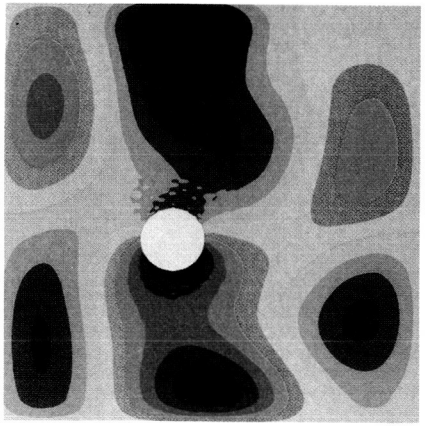

$\dot{\varphi}_1/|\dot{\varphi}_1|_{max}$

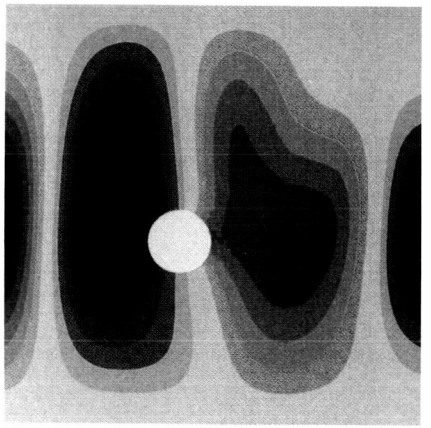

$\dot{\varphi}_2/|\dot{\varphi}_2|_{max}$

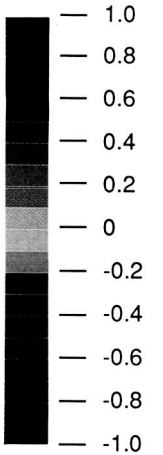




(c) Linear velocity components.

Figure 5. Continued.

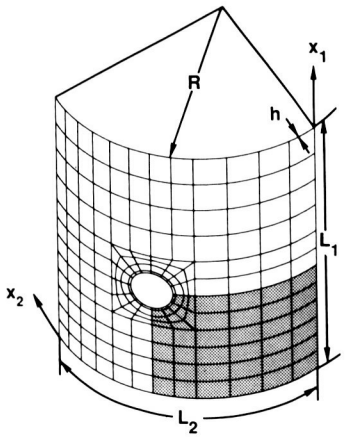


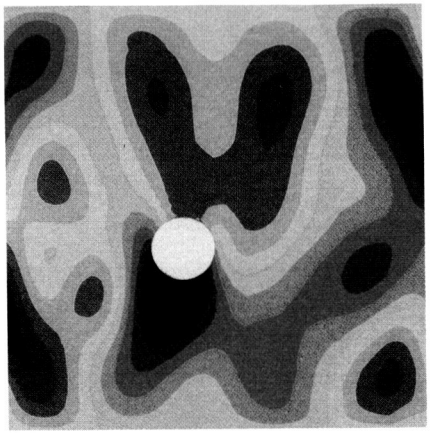

$\dot{u}_1/|\dot{u}_1|_{max}$

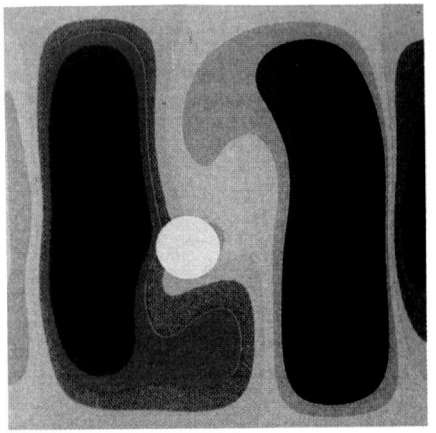

$\dot{u}_2/|\dot{u}_2|_{max}$

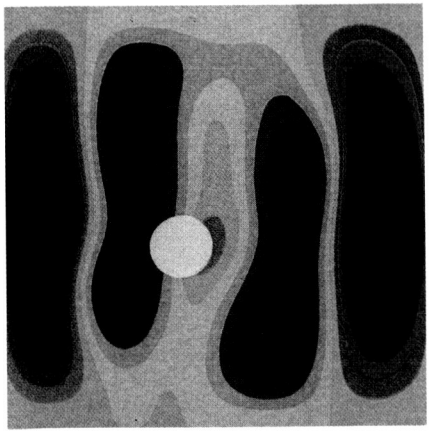

$\dot{w}/|\dot{w}|_{max}$

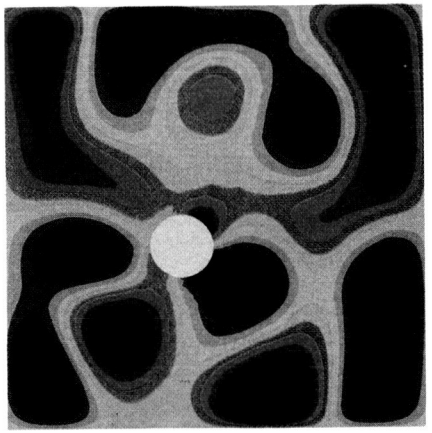

$\dot{\varphi}_1/|\dot{\varphi}_1|_{max}$

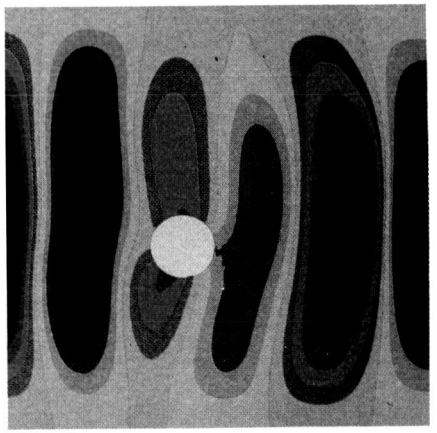

$\dot{\varphi}_2/|\dot{\varphi}_2|_{max}$

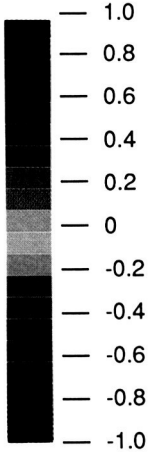




(d) Nonlinear velocity components.

Figure 5. Concluded.

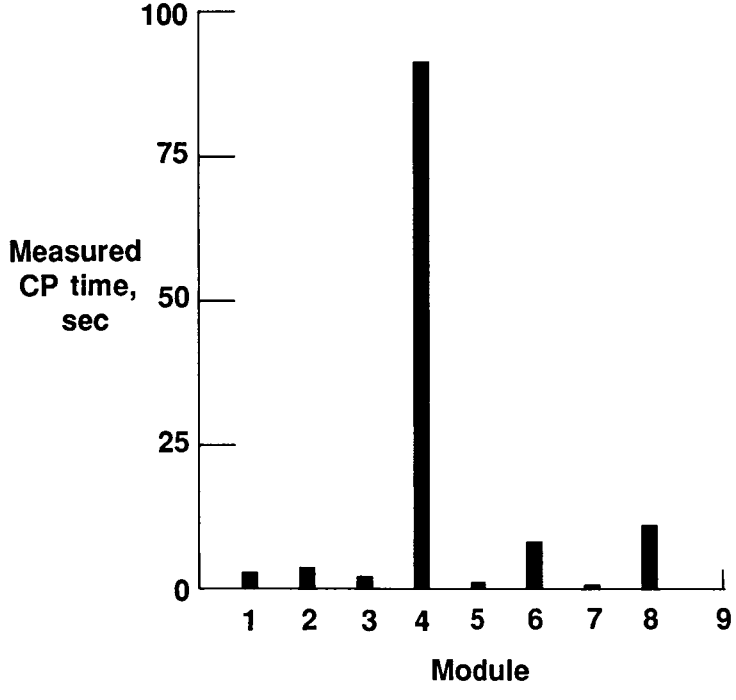


| Module | Description* | |
|---|---|---|
| 1 | Preprocessing (steps 1 and 2) | |
| 2 | Generation of nonlinear elemental contributions and assembly of right-hand side (steps 5,6, and 8) | |
| 3 | Eliminating stresses from left-hand side and assembly of left-hand side (step 7) | |
| 4 | Incorporation of boundary conditions and decomposition of preconditioning matrices (step 10) | |
| 5 | Eliminating stresses from right-hand side | (steps 11 and 12) |
| 6 | Back solve | |
| 7 | Recovery of stresses | |
| 8 | Step lengths and conjugate search directions | |
| 9 | Convergence checks (step 13) | |

*See table I for steps.

Figure 6. Measured CP times on CRAY X-MP/416 (UNICOS 3.0.8 operating system, CFT compiler version 1.15 BF2). Laminated anisotropic composite panel with off-center circular cutout subjected to uniform normal loading $p_o = -50\,000$ Pa (see fig. 3); times represent total CP times on 1 CPU for first 10 time steps.

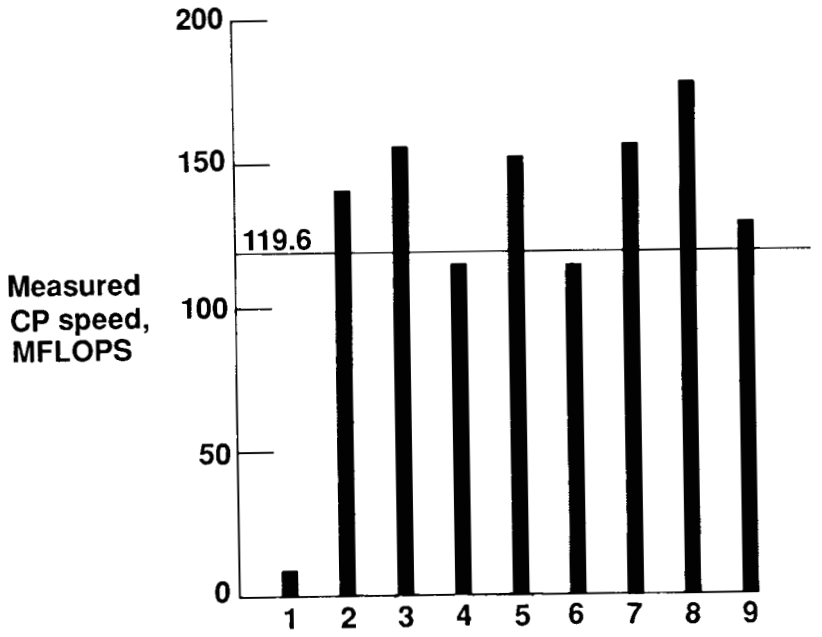


| Module | Description* |
|---|---|
| 1 | Preprocessing (steps 1 and 2) |
| 2 | Generation of nonlinear elemental contributions and assembly of right-hand side (steps 5,6, and 8) |
| 3 | Eliminating stresses from left-hand side and assembly of left-hand side (step 7) |
| 4 | Incorporation of boundary conditions and decomposition of preconditioning matrices (step 10) |
| 5 | Eliminating stresses from right-hand side (steps 11 and 12) |
| 6 | Back solve (steps 11 and 12) |
| 7 | Recovery of stresses (steps 11 and 12) |
| 8 | Step lengths and conjugate search directions (steps 11 and 12) |
| 9 | Convergence checks (step 13) |

*See table I for steps.

Figure 7. Measured CP speed on one CPU of CRAY X-MP/416 (UNICOS 3.0.8 operating system, CFT compiler version 1.15 BF2). Laminated anisotropic composite panel with off-center circular cutout subjected to uniform normal loading $p_o = -50\,000$ Pa (see fig. 3); speed represents sustained CP speed at one CPU during first 10 time steps.

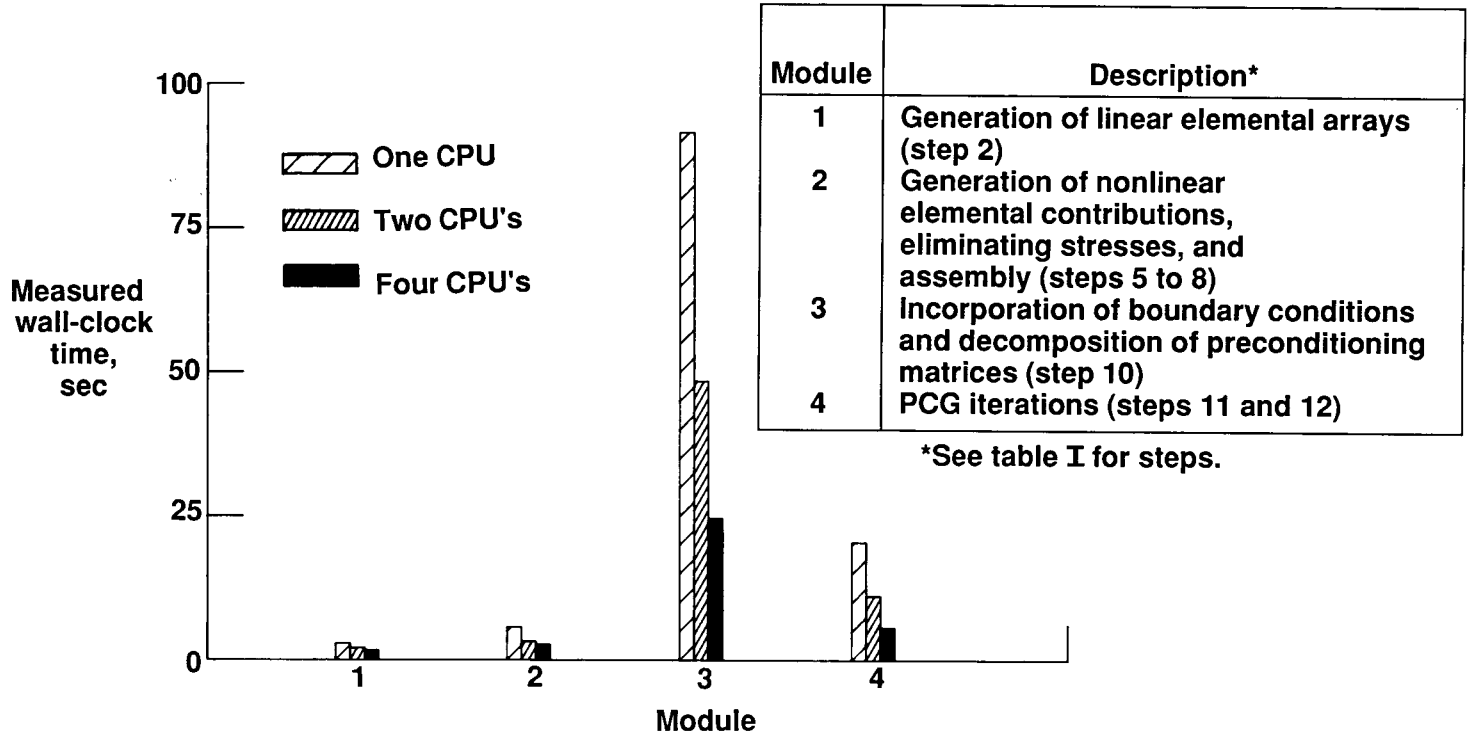


Figure 8. Measured wall-clock times on CRAY X-MP/416 (UNICOS 3.0.8 operating system, CFT compiler version 1.15 BF2). Laminated anisotropic composite panel with off-center circular cutout subjected to uniform normal loading $p_o = -50\,000$ Pa (see fig. 3); times represent total wall-clock times for first 10 time steps.

NASA
National Aeronautics and Space Administration

# Report Documentation Page

| 1. Report No. | 2. Government Accession No. | 3. Recipient's Catalog No. |
|---|---|---|
| NASA TP-2850 | | |

| 4. Title and Subtitle | 5. Report Date |
|---|---|
| Partitioning Strategy for Efficient Nonlinear Finite Element Dynamic Analysis on Multiprocessor Computers | January 1989 |
| | 6. Performing Organization Code |
| 7. Author(s) | 8. Performing Organization Report No. |
| Ahmed K. Noor and Jeanne M. Peters | L-16476 |
| 9. Performing Organization Name and Address | 10. Work Unit No. |
| NASA Langley Research Center<br>Hampton, VA 23665-5225 | 505-63-01-11 |
| | 11. Contract or Grant No. |
| 12. Sponsoring Agency Name and Address | 13. Type of Report and Period Covered |
| National Aeronautics and Space Administration<br>Washington, DC 20546-0001 | Technical Paper |
| | 14. Sponsoring Agency Code |

15. Supplementary Notes

Ahmed K. Noor and Jeanne M. Peters: The George Washington University, Joint Institute for Advancement of Flight Sciences, Langley Research Center, Hampton, Virginia.

The present research was supported by NASA Grant NAG1-730 and Air Force Office of Scientific Research Grant AFOSR-88-0136.

16. Abstract

A computational procedure is presented for the nonlinear dynamic analysis of unsymmetric structures on vector multiprocessor systems. The procedure is based on a novel hierarchical partitioning strategy in which the response of the unsymmetric structure at any time instant is approximated by a linear combination of symmetric and antisymmetric response vectors, each obtained by using only a fraction of the degrees of freedom of the original finite element model. The three key elements of the procedure which result in a high degree of concurrency throughout the solution process are (1) mixed (or primitive variable) formulation with independent shape functions for the different fields; (2) operator splitting or restructuring of the discrete equations at each time step to delineate the symmetric and antisymmetric vectors constituting the response; and (3) two-level iterative process for generating the response of the structure. An assessment is made of the effectiveness of the procedure on the CRAY X-MP/4 computers.

| 17. Key Words (Suggested by Authors(s)) | 18. Distribution Statement |
|---|---|
| Nonlinear dynamic analysis<br>Parallel processing<br>Hierarchical partitioning<br>Multiprocessor computers<br>Symmetry transformations<br>Operator splitting<br>Mixed formulations<br>Iterative techniques | Unclassified—Unlimited<br><br>Subject Category 39 |

| 19. Security Classif.(of this report) | 20. Security Classif.(of this page) | 21. No. of Pages | 22. Price |
|---|---|---|---|
| Unclassified | Unclassified | 38 | A03 |



For sale by the National Technical Information Service, Springfield, Virginia 22161-2171